Elsevier Editorial System(tm) for Computer Networks
Manuscript Draft

Manuscript Number:

Title: Advanced Mobility Management for Reduced Interference and Energy Consumption in the Two-tier LTE-Advanced Network

Article Type: Regular Paper

Keywords: LTE-Advanced; femtocells; energy efficiency; interference management; signaling; handover decision algorithm

Corresponding Author: Mr. Dionysis Xenakis,

Corresponding Author's Institution: University of Athens

First Author: Dionysis Xenakis

Order of Authors: Dionysis Xenakis; Nikos Passas, Dr; Lazaros F Merakos, Dr; Christos Verikoukis, Dr

Abstract: Femtocell deployment will play a key role for the wide adoption of LTE-Advanced, as it brings the access network closer to the end user in a cost-effective manner. This disruptive communication paradigm, however, necessitates the employment of advanced interference and mobility management to cope with the comparably denser yet unplanned network layout. This paper describes an advanced mobility management approach for the two-tier LTE-Advanced network, aiming to resourcefully utilize the femtocell superior characteristics in an energy-efficient and interference-aware manner. The key features of the proposed approach are a) the exchange and utilization of standard signal quality measurements during the handover decision phase, to accurately estimate the mean user equipment (UE) transmit power on a per candidate cell basis, and b) the use of a novel handover decision algorithm that jointly considers the impact of interference, power consumption, and user mobility. A comprehensive analysis of the required network signaling is provided, while extensive simulation results demonstrate that compared to existing approaches, the proposed approach attains improved performance at the cost of moderate increase of network signaling.

Advanced Mobility Management for Reduced Interference and Energy Consumption in the Two-tier LTE-Advanced Network

Dionysis Xenakis[†], Nikos Passas[†], Lazaros Merakos[†], Christos Verikoukis[*]

[†]Dept. of Informatics and Telecommunications
University of Athens, Greece
{nio | passas | merakos}@di.uoa.gr

[*]Telecommunications Technological Centre of Catalonia
Barcelona, Spain
cveri@cttc.es

Abstract – Femtocell deployment will play a key role for the wide adoption of LTE-Advanced, as it brings the access network closer to the end user in a cost-effective manner. This disruptive communication paradigm, however, necessitates the employment of advanced interference and mobility management to cope with the comparably denser yet unplanned network layout. This paper describes an advanced mobility management approach for the two-tier LTE-Advanced network, aiming to resourcefully utilize the femtocell superior characteristics in an energy-efficient and interference-aware manner. The key features of the proposed approach are a) the exchange and utilization of standard signal quality measurements during the handover decision phase, to accurately estimate the mean user equipment (UE) transmit power on a per candidate cell basis, and b) the use of a novel handover decision algorithm that jointly considers the impact of interference, power consumption, and user mobility. A comprehensive analysis of the required network signaling is provided, while extensive simulation results demonstrate that compared to existing approaches, the proposed approach attains improved performance at the cost of moderate increase of network signaling.

Keywords **– LTE-Advanced; femtocells; energy efficiency; interference management; signaling; handover decision algorithm;**

Corresponding author:
Dionysis Xenakis
Dept. of Informatics and Telecommunications
University of Athens
15784, Athens, Greece
Tel: +302107275123
Fax: +302107275601
Email: nio@di.uoa.gr

1. INTRODUCTION

Release 10 of the 3rd Generation Partnership Project (3GPP) for the Long Term Evolution (LTE) system, also known as LTE-Advanced (LTE-A), fulfills and even surpasses the International Mobile Telecommunications (IMT)-Advanced requirements set by the International Telecommunication Union (ITU) [1], [2]. In LTE-A, a transmission to/from a mobile terminal can utilize up to five component carriers with carrier aggregation (CA), i.e., a deployment bandwidth of up to 100MHz, where each component carrier uses the Release 8 structure for backwards compatibility. LTE-A supports advanced spatial multiplexing, using up to eight-layer multiple-input multiple-output (MIMO) for the downlink (DL) and up to four-layer MIMO for the uplink (UL), which combined with CA leads to a peak data rate of 1Gbps and 0.5Gbps for the DL and UL directions, respectively. To further improve spectral efficiency, LTE-A enables enhanced single-cell DL multiuser MIMO support, while to lower the interference at User Equipments (UEs) located close to multiple evolved Node Bs (eNBs), the standard provisions for coordinated multipoint (CoMP) transmissions. A wide range of heterogeneous deployments are also supported by the LTE-A standard, mainly including picocells, femtocells, and relays, with the aim to extend network coverage, increase system capacity, and lower transmit power [3].

Femtocells can play a key role for wide adoption of LTE-A, as they bring the access network closer to the user in a cost-effective manner [4]. Femtocells, a.k.a., Home eNBs, are short-range, low-cost, consumer-deployed cellular access points, which interconnect standard user equipment (UE) to the mobile operator network via the end user's broadband access backhaul. Although femtocells typically support up to a few users, they embody the functionality of a regular base station which operates in the mobile operator's licensed band. Femtocells can substantially enhance the user-perceived Quality of Service (QoS) and greatly improve the energy saving potential for the network nodes at the cost of employing more sophisticated interference and mobility management procedures.

The need for advanced interference and mobility management originates from a) the unplanned femtocell deployment, b) the short femtocell radius, d) the denser network layout, and d) the employment of access control [5]. The unplanned deployment pattern increases the radio-frequency (RF) interference at the LTE-A network nodes in an unpredicted manner, and complicates the mobility management procedure, e.g., the serving LTE-A cell is unable to provide a complete neighbor cell list to the UEs. On the other hand, the short femtocell radius and the denser network layout increase the number of handovers (HOs) in the system and enlarge the number of candidate cells, compromising seamless connectivity and increasing the network signaling load. Finally, access control may result in severely degraded Signal to Interference plus Noise Ratio (SINR) performance under certain interference scenarios, e.g., when an LTE-A user is not a member of a Closed Subscriber Group (CSG) femtocell in proximity [5].

Even though femtocell deployment comprises several technical challenges, it is expected to significantly reduce the energy expenditure for both the UEs and the LTE-A network. As reported in [6], if a femtocell tier is deployed, then both the mobile terminals and the cellular stations can reduce their transmit power by four to eight orders of magnitude. In-band macrocell and femtocell coexistence, however, increases the RF interference, which in turn degrades the system capacity per-tier and reduces the energy saving potential [7]. Self-optimization is another femtocell feature that leads to further energy savings. For example, the proposed dynamic pilot transmission mechanism in [8] is shown to improve the femtocell energy efficiency and reduce the occurrence of mobility events for passing outdoor users. In conclusion, even though femtocell deployment natively enhances the energy saving potential at the access network nodes, the actual energy consumption gain strongly depends on the interference and mobility management decisions employed.

This paper describes an advanced mobility management approach for the two-tier LTE-A network, aiming to lower the interference and energy consumption at the network nodes, while sustaining seamless connectivity and a prescribed mean SINR target. To achieve this, a two-step HO decision

algorithm is proposed, which a) excludes a subset of candidate cells that can compromise sustained wireless connectivity, and b) selects the candidate cell with the minimum required mean UE transmit power for the prescribed SINR target. Both these steps are employed by adapting the HO Hysteresis Margin (HHM) according to standard LTE-A signal quality measurements, performed either by the UE or the candidate cells. The required network signaling procedure is thoroughly investigated and two different signaling approaches are identified, depending on whether an LTE-A network entity maintains and disseminates these signal quality measurements, or not. Based on the Small Cell Forum evaluation methodology in [9], it is shown that the proposed algorithm attains a significant reduction of transmit power and interference, as well as substantial improvement of system capacity and energy consumption per bit, at the cost of moderately increased network signaling load.

The remainder of this paper is organized as follows. Section 2 summarizes related works, and highlights the key aspects and contributions of this paper. Section 3 describes the adopted system model, and discusses the predominant strongest cell (SC) HO decision algorithm in the context of LTE-A. The proposed algorithm presented in Section 4, while two different signaling procedures for employing it are thoroughly investigated in Section 5. Section 6 includes extensive system-level simulation results and Section 6 concludes this paper.

2. RELATED WORK

The LTE-A standard describes a wide range of technical improvements for the LTE system, mainly including carrier aggregation [10], advanced multi-antenna techniques [11], enhanced support for heterogeneous deployments [2], [3], and relaying [12]. The key features and a series of open issues for femtocell deployment are summarized in [4], while a more comprehensive analysis is provided in [13]. A performance analysis is conducted in [14], to assess the per-tier outage probability in co-channel femtocell deployments owing to cross-tier interference.

Current literature includes various approaches for handling interference in femtocell networks [15]-[24]. A wide range of interference coordination and cancellation techniques are summarized in [15], with the emphasis given to the LTE system. To mitigate cross-tier interference in the two-tier network, advanced radio resource allocation and power control schemes are proposed in [16]-[19]. Focusing on the LTE-A system with multi-hop relaying, the performance of semi-static interference coordination schemes for radio resource allocation and power control, in both the frequency and time domain, is demonstrated in [20]. The achievable SINR performance of the macrocell tier is investigated in [21], with respect to the number of femtocells deployed in the two-tier network. A utility-based SINR adaptation algorithm is subsequently proposed for the femtocell nodes, aiming to mitigate the interference caused to the macrocell tier in a distributed manner. Two interference mitigation strategies are proposed in [22], which suppress the cross-tier interference to the macrocell tier by adjusting the maximum transmit power at the femtocell users. Based on decentralized Q-learning and knowledge dissemination among the femtocell stations, a self-optimization approach is described in [23], which is shown to sustain an improved macrocell capacity and SINR performance compared to an independent learning approach. An orthogonal random beamforming-based strategy is proposed in [24], aiming to reduce the cross-tier interference in the two-tier network, increase the spatial opportunity of the femtocell nodes, and mitigate the degradation to the macrocell capacity. Analytical and numerical results illustrate that combined with opportunistic channel selection and distributed power control, the proposed strategy sustains the macrocell throughput and reduces the mean transmit power at the femtocell nodes. Different from the approaches above, this paper describes a novel interference mitigation approach based on the employment of interference-aware HO decision making.

Current literature also includes various algorithms and studies for the HO decision phase in the two-tier network [25]-[33]. Two different sets of speed and Received Signal Strength (RSS) based HO decision rules are proposed in [25], to minimize the HO probability in the two-tier network. The

proposed rules are shown to increase the user-perceived throughput in high speed UEs, and reduce the HO probability compared to a soft HO decision approach. The authors in [26] propose two different HO decision strategies depending on the traffic type of the user. For non real-time traffic, a SC-based HO decision strategy is proposed, while for real-time traffic, the proposed strategy consists of executing an outband femtocell HO only when the minimum required RSS for service continuity is reached. Although the employment of these strategies is shown to reduce the number of HOs in the system, the impact of the consequential RF interference on the user-perceived throughput is not investigated. An adaptive HO Hysteresis Margin (HHM) approach is presented in [27], where the HHM value is adapted according to the estimated path loss between the UE and the target cell. It is shown that even though a large HHM lowers the number of unnecessary HOs, it simultaneously degrades the throughput performance. Aiming to sustain a low outage probability for the LTE-A users, the authors in [28] propose a fractional soft HO decision algorithm, which takes into account the user traffic type and uses the feature of carrier aggregation. Even though theoretical and simulation results illustrate low outage probability, the performance of the proposed algorithm in terms of energy consumption and interference at the LTE-A nodes is not discussed. To mitigate cross-tier interference and reduce the number of HOs in the network, the work in [29] is based on the concept of intra-cell HOs which, however, is closer to radio resource management rather than HO decision making. The proposal in [30] allows for an inbound HO to femtocells depending on the traffic type and the current user mobility status. A variant of this algorithm is presented in [31], with the addition of a simple analysis regarding the required signaling overhead based on the work in [32]. Founded on simulation results, the work in [33] concludes that more efficient interference coordination and HO execution procedures can be employed, if the communication between the macrocell and the femtocell tiers is performed through the X2, rather than the S1 interface [1]. In our previous works in [34]-[35], we have proposed the exchange and utilization of standard measurements for reducing the power consumption of the UEs in the two-tier LTE system. Nevertheless, further work is required towards lowering the negative impact of user mobility on the HO probability performance, as well as assessing the required signaling procedures and overheads required for deploying the proposed HO decision algorithms.

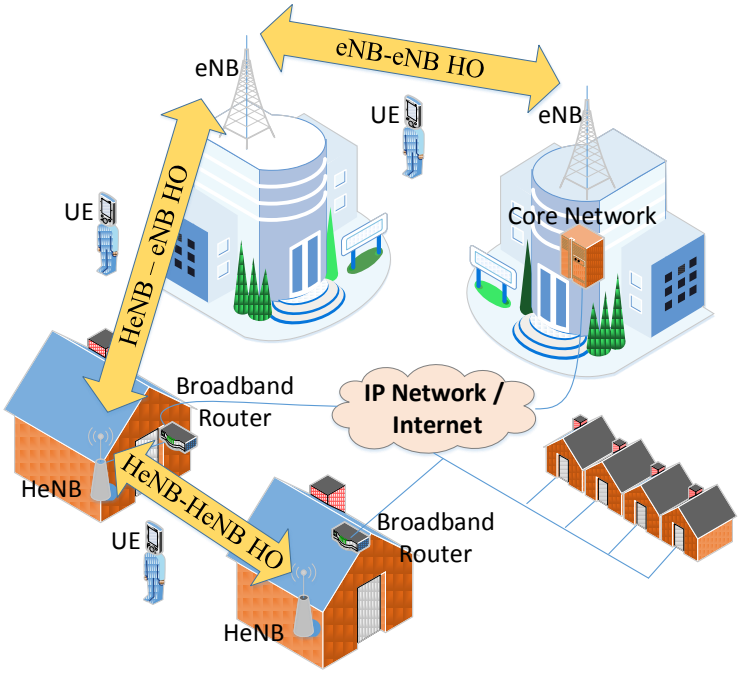

Figure 1: Two-tier LTE-A network and type of HOs

To summarize, current HO decision algorithms emphasize on reducing the number of HOs in the two-tier network mainly based on user mobility and traffic type criteria. In most of the cases, the

impact of the proposed algorithms on the UE energy consumption, the RF interference, and the network signaling load, is not investigated. On the other hand, existing approaches mainly focus on the inter-tier HO decision scenario, and assume the employment of the SC algorithm for the intra-tier HO scenario, i.e., eNB-to-eNB and HeNB-to-HeNB HOs (Fig. 1). The SC HO decision algorithm, however, does not take into account the actual transmit power on the Reference Signals (RS) of the candidate cells, neither it takes into account the RF interference at the cell sites, which are both expected to diverge from site to site in the LTE-A network, owing to the unplanned deployment and the self-optimization mechanisms. As a result, the employment of the interference-agnostic SC algorithm is expected to degrade the SINR performance, compromise seamless connectivity, increase the outage probability and enlarge the HO signaling.

In this work we jointly consider the impact of interference, power consumption, and user mobility during the HO decision phase in the two-tier LTE-A network. A strong innovation of this work is the exchange and utilization of standard LTE-A measurements to accurately estimate the mean UE transmit power on a per candidate cell basis, given a prescribed mean SINR target. The exclusion of candidate LTE-A cells which can compromise wireless connectivity, and the incorporation of the user's prescribed SINR target during the mean UE transmit power estimation, are two more important features of the proposed algorithm towards sustained wireless connectivity, enhanced QoS support, and reduced outage probability. Finally, the comprehensive description of the network signaling procedure required for employing the proposed algorithm, guarantees backwards compatibility with LTE-A and provides insights for advanced interference and mobility management in the two-tier network.

3. SYSTEM MODEL

3.1 System Description

An LTE-A network is considered, operating in the band set $\boldsymbol{N} \coloneqq \{1, \dots, N\}$. Let $\boldsymbol{R_n} \coloneqq \{1, \dots, R_n\}$ denote the set of Resource Blocks (RB) in band $n \in \boldsymbol{N}$, $\boldsymbol{C_n}$ the set of cells operating in band n, including both eNBs and Home eNBs (HeNBs), and $\boldsymbol{U_n}$ the set of active users connected to a cell in $\boldsymbol{C_n}$. For a tagged user u, let $\overline{\gamma}^{u}_{target}$ denote the prescribed mean SINR target for attaining the required QoS, $RSRP^{u}_{min}$ the minimum required RSRP value for sustaining wireless connectivity with the network, and $\boldsymbol{L_u} \subseteq \bigcup_{n \in \boldsymbol{N}} \boldsymbol{C_n}$ the set of candidate and accessible LTE-A cells identified during the network discovery phase. Given two network nodes x and y, which can be either LTE-A cells or UEs, let $\overline{P}^{T}_{x}$ denote the transmit power of node x, $\left(\overline{\sigma}^{T}_{x}\right)^2$ the noise power in node x, and $\overline{h}^{T}_{x \to y}$ the channel gain between nodes x and y, all averaged within the operating bandwidth of the respective nodes over the time interval T. Accordingly, the mean UL SINR between user $u \in \boldsymbol{U_n}$ and cell $s \in \boldsymbol{C_n}$ for the time interval T is given as follows:

$$\overline{\gamma}^{T}_{u \to s} = \frac{\overline{P}^{T}_{u} \cdot \overline{h}^{T}_{u \to s}}{\sum_{c \in \boldsymbol{C_n} - \{s\}} \overline{P}^{T}_{c} \cdot \overline{h}^{T}_{c \to s} + \sum_{u' \in \boldsymbol{U_n} - \{u\}} \overline{P}^{T}_{u'} \cdot \overline{h}^{T}_{u' \to s} + \left(\overline{\sigma}^{T}_{s}\right)^2} \qquad (1)$$

where the numerator corresponds to the receive signal strength for user u in the serving cell s, the first and the second terms of the denominator to the interference caused by cells and users operating in-band, respectively, and the third term to the noise power at cell s. By using Eq. (1) and taking into account the requirement for sustaining the prescribed mean SINR target $\overline{\gamma}^{u}_{target}$, the mean UE transmit power of user u for a candidate cell $c \in \boldsymbol{L_u}$ can be estimated as follows:

$$\overline{P}^{T}_{u \to c} = \frac{\overline{\gamma}^{u}_{target} \cdot \left(\sum_{c' \in \boldsymbol{C_n} - \{c\}} \overline{P}^{T}_{c'} \cdot \overline{h}^{T}_{c' \to c} + \sum_{u' \in \boldsymbol{U_n} - \{u\}} \overline{P}^{T}_{u'} \cdot \overline{h}^{T}_{u' \to c} + \left(\overline{\sigma}^{T}_{c}\right)^2\right)}{\overline{h}^{T}_{u \to c}} \qquad (2)$$

Note that the positive impact of handing over to cell $c \in \boldsymbol{L_u}$, in terms of lower interference, is incorporated in Eq. (2) by omitting the interference caused to cell c by the ongoing user connection with the current serving cell s, i.e., $\overline{P}_u^T \cdot \overline{h}_{u \to s}^T$. Eq. (2) can also be used to estimate the mean UE power consumption of the tagged user u in cell c, owing to transmit power.

Table I: Signal quality measurements for the LTE-A system [36]

Measurement	Measured by	Notation
Reference Signal Received Power (RSRP)	UE	$RSRP_{c \to u}^T$
E-UTRAN Carrier Received Signal Strength Indicator (RSSI)	UE	$RSSI_{c \to u}^T$
Reference Signal Received Quality (RSRQ)	UE	$RSRQ_{c \to u}^T$
Downlink Reference Signal Transmitted Power (DL RS Tx)	E-UTRAN	$P_{c,RS}^T$
Received Interference Power (RIP) over the RB set $\boldsymbol{R_n}$	E-UTRAN	$\overline{I}_c^T$

The LTE-A standard describes a wide set of signal quality measurements for the LTE-A access network and the UEs in [36], which can be utilized to accurately estimate the mean UL SINR in Eq. (1) and the mean UE transmit power in Eq. (2). The LTE-A measurements used in this paper, along with the respective notation for a tagged user u, cell c, and time interval T, are summarized in Table I. Note that the Received Interference Power (RIP) measurement in Table I, denoted by $\overline{I}_c^T$, corresponds to the linear average of the RIP measurements performed over the utilized RB of cell c [36]. To the remainder of this paper, it is assumed that for all the UEs connected to it, each serving cell has a consistent list of candidate cells and signal quality measurements describing their status. Even though the acquisition of these measurements is described in Section 4, the network discovery phase is outside the scope of this paper.

3.2 Strongest Cell Handover Decision Algorithm

In the context of LTE-A, the SC HO decision algorithm consists of handing over to the candidate cell with the highest RSRP status, which also exceeds over the RSRP status of the serving cell plus a policy-defined HHM for a time period namely the Time To Trigger (TTT) [37]. The HHM is typically introduced to mitigate frequency-related propagation divergences, and the negative impact of the ping-pong effect. Based on the system model description in Section 3.1, the SC HO decision algorithm can be summarized as follows:

$$\arg\max_{c \in \boldsymbol{L_u}} RSRP_{c \to u,(dB)}^{TTT} \coloneqq \left\{ c \middle| RSRP_{c \to u,(dB)}^{TTT} > RSRP_{s \to u,(dB)}^{TTT} + HHM_{c,(dB)} \right\} \quad (3)$$

where $HHM_{c,(dB)}$ corresponds to the HHM for cell $c \in \boldsymbol{L_u}$, and $X_{(dB)}$ to the value of X in decibels (dB). Taking into account the definition of the RSRP measurement [36], it follows that:

$$RSRP_{c \to u}^{TTT} = P_{c,RS}^{TTT} \cdot \overline{h}_{c \to u}^{TTT} \quad (4)$$

By substituting Eq. (4) to Eq. (3), it can be shown that the SC algorithm facilitates mobility towards candidate cells with higher RS transmit power, and/or improved channel gain. However, in order for the SC algorithm to improve the channel gain for the tagged LTE-A link (Eq. 4), comparable RS transmit powers should be radiated among the candidate cells. However, this is not in effect in the two-tier LTE-A network provided that a) eNBs typically radiate higher RS transmit power compared to HeNBs, and b) femtocell self-optimization can result in different RS transmit powers between the HeNBs. In addition, the SC algorithm does not necessarily improve the SINR performance (Eq. (1), (2)) given that divergent interference levels are expected at the LTE-A cell sites owing to the unplanned deployment. The SC algorithm's unawareness on the actual RS transmit power and the

interference level at the cell sites, is also expected to increase the UE transmit power, which in turn rises the interference level network-wide and exhausts the UE battery lifetime. The value of the HHM parameter is another open issue for the SC algorithm.

4. HANDOVER DECISION ALGORITHM

Based on the discussion in Section 3, this section describes an advanced handover decision algorithm, which is based on the employment of interference-aware and energy-efficient HO decision making. The proposed algorithm utilizes standard LTE-A measurements a) to mitigate the negative impact of user mobility and b) minimize the UE transmit power given the mean SINR target. The former is achieved by avoiding HOs to cells that can compromise wireless connectivity, while the latter by estimating the UE transmit power on the remainder cells and handing over to the one with the minimum requirements. The rest of this section is organized as follows. Section 4.1 describes a methodology for sustaining wireless connectivity, while Section 4.2 describes a HO decision criterion for identifying the cell requiring the minimum UE transmit power. These procedures are integrated to the proposed algorithm in Section 4.3.

4.1 Sustained wireless connectivity

Let $\overline{P}_{max}^{x,T}$ denote the maximum allowed mean transmit power for node x, which corresponds either to the maximum transmit power of the target cell, or the UE power class, or a maximum transmit power constraint adapted with respect to interference mitigation criteria, e.g., as in [22]. Using Eq. (4) under the assumption of a symmetric channel gain, the mean UL channel gain between user u and cell c can be estimated as follows:

$$\overline{h}_{u\to c}^{T} \cong \overline{h}_{c\to u}^{T} = \frac{RSRP_{c\to u}^{T}}{P_{c,RS}^{T}} \quad (5)$$

Let $\overline{h}_{c\to u,min}^{T}$ denote the minimum required channel gain for sustaining wireless connectivity between user u and cell c. Taking into account the minimum required RSRP value for sustaining wireless connectivity ($RSRP_{min}^{u}$), and the maximum allowed mean transmit power for user u and cell c, i.e., $\overline{P}_{max}^{u,T}$ and $\overline{P}_{max}^{c,T}$, respectively, the $\overline{h}_{c\to u,min}^{T}$ parameter can be estimated as follows:

$$\overline{h}_{c\to u,min}^{T} = \frac{RSRP_{min}^{u}}{\min\left(\overline{P}_{max}^{u,T}, \overline{P}_{max}^{c,T}\right)} \quad (6)$$

Using Eq. (5) and (6) for the HO decision time horizon $T = TTT$ and under the condition for sustaining wireless connectivity $\overline{h}_{u\to c}^{TTT} > \overline{h}_{c\to u,min}^{TTT}$, the candidate cell set is limited as follows:

$$\boldsymbol{M_u} := \left\{ c \middle| RSRP_{c\to u,(dB)}^{TTT} > RSRP_{min,(dB)}^{u} + P_{c,RS,(dB)}^{TTT} - \min\left(\overline{P}_{max}^{u,TTT}, \overline{P}_{max}^{c,TTT}\right), and\ \mathrm{c} \in \boldsymbol{L_u} \right\} \quad (7)$$

4.2 HO decision criterion for reduced mean UE transmit power

Having identified the candidate cell set that guarantees sustained wireless connectivity, this section describes a novel methodology for estimating the tagged user's mean UE transmit power on a per candidate cell basis, with respect to the prescribed mean SINR target and standard LTE-A measurements. The incorporation of the prescribed SINR target provisions for the supported QoS, while the utilization of standard LTE-A measurements provides an accurate estimation on the required mean UE transmit power. In the following, it is assumed that the tagged user u receives service from cell s, which has consistent measurements describing the status of every candidate cell $\mathrm{c} \in \boldsymbol{M_u}$ over the time interval $T = TTT$.

By taking into account the RIP measurement definition in [36], it follows that:

$$\overline{I}_c^T = \left(\sum_{c' \in \boldsymbol{C_n} - \{c\}} \overline{P}_{c'}^T \cdot \overline{h}_{c' \to c}^T + \sum_{u' \in \boldsymbol{U_n}} \overline{P}_{u'}^T \cdot \overline{h}_{u' \to c}^T + \left(\overline{\sigma}_c^T\right)^2\right) \quad (8)$$

By using Eq. (2), (5), and (8), it can be readily shown that the mean UE transmit power for the current serving cell s can be estimated by Eq. (9).

$$\overline{P}_u^T = \frac{\overline{\gamma}_{target}^u \cdot P_{s,RS}^T \cdot \overline{I}_s^T}{RSRP_{s \to u}^T} \quad (9)$$

Under the same viewpoint, the mean UE transmit power for a candidate cell $c \in \boldsymbol{M_u}$ can be estimated as follows:

$$\overline{P}_{u \to c}^T = \begin{cases} \frac{\overline{\gamma}_{target}^u \cdot P_{c,RS}^T \cdot \left(\overline{I}_c^T - \overline{P}_u^T \cdot \overline{h}_{u \to c}^T\right)}{RSRP_{c \to u}^T}, & if\ c, s \in \boldsymbol{C_n} \\ \frac{\overline{\gamma}_{target}^u \cdot P_{c,RS}^T \cdot \overline{I}_c^T}{RSRP_{c \to u}^T}, & otherwise \end{cases} \quad (10)$$

where the condition $c, s \in \boldsymbol{C_n}$ is introduced to include the interference caused by the ongoing user link with cell s, i.e., $\overline{P}_u^T \cdot \overline{h}_{u \to s}^T$, if cells c and s operate in the same band. Let us now focus on the HO decision at the serving cell. A HO to the candidate cell $c \in \boldsymbol{M_u}$ is expected to lower the mean UE transmit power if the condition $\overline{P}_{u \to s}^{TTT} > \overline{P}_{u \to c}^{TTT}$ is met. By using Eq. (10) and taking the values in dB, it can be readily shown that this condition can be rearranged as follows:

$$RSRP_{c \to u,(dB)}^{TTT} > RSRP_{s \to u,(dB)}^{TTT} + HHM_{c,(dB)} \quad (11)$$

where the parameter $HHM_{c,(dB)}$ is adapted according to Eq. (12).

$$HHM_{c,(dB)} = \begin{cases} 10 \log \frac{P_{c,RS}^{TTT} \cdot \left(\overline{I}_c^{TTT} - \frac{\overline{\gamma}_{target}^u \cdot P_{s,RS}^{TTT} \cdot \overline{I}_s^{TTT}}{RSRP_{s \to u}^{TTT}} \cdot \frac{RSRP_{c \to u}^{TTT}}{P_{c,RS}^{TTT}}\right)}{P_{s,RS}^{TTT} \cdot \overline{I}_s^{TTT}} & c, s \in \boldsymbol{C_n} \\ 10 \log \frac{P_{c,RS}^{TTT} \cdot \overline{I}_c^{TTT}}{P_{s,RS}^{TTT} \cdot \overline{I}_s^{TTT}} & otherwise \end{cases} \quad (12)$$

Eq. (11) can be used as a HO decision criterion for lowering the mean UE transmit power in the two-tier LTE-A network. The latter is achieved by introducing the adaptive HHM of Eq. (12) in the standard HO decision procedure as follows:

$$\arg\max_{c \in \boldsymbol{M_u}} RSRP_{c \to u,(dB)}^{TTT} := \left\{c \middle| RSRP_{c \to u,(dB)}^{TTT} > RSRP_{s \to u,(dB)}^{TTT} + HHM_{c,(dB)}\right\} \quad (13)$$

4.3 Proposed HO decision algorithm

The proposed HO decision algorithm integrates the methodology for sustained wireless connectivity in Section 4.1, and the HO decision criterion for reduced mean UE transmit power in Section 4.2. To further reduce the HO failure probability, the proposed algorithm takes into account the resource availability on the candidate LTE-A cells, while to cope with critical LTE-A events, the decision time horizon of the proposed algorithm can be limited to a prescribed time duration, denoted by T_{max}. Finally, to deal with potential network signaling delay during the HO context acquisition procedure, the proposed algorithm handles the candidate cell list as a queue structure, which allows prioritized evaluation of the candidate cells with known status. Note that the required HO decision context consists of a) the operating frequency and bandwidth of the candidate cells, b) their current capacity value [38], c) the signal quality measurements in Table I, and d) the maximum allowed mean transmit power for user u and the candidate cells.

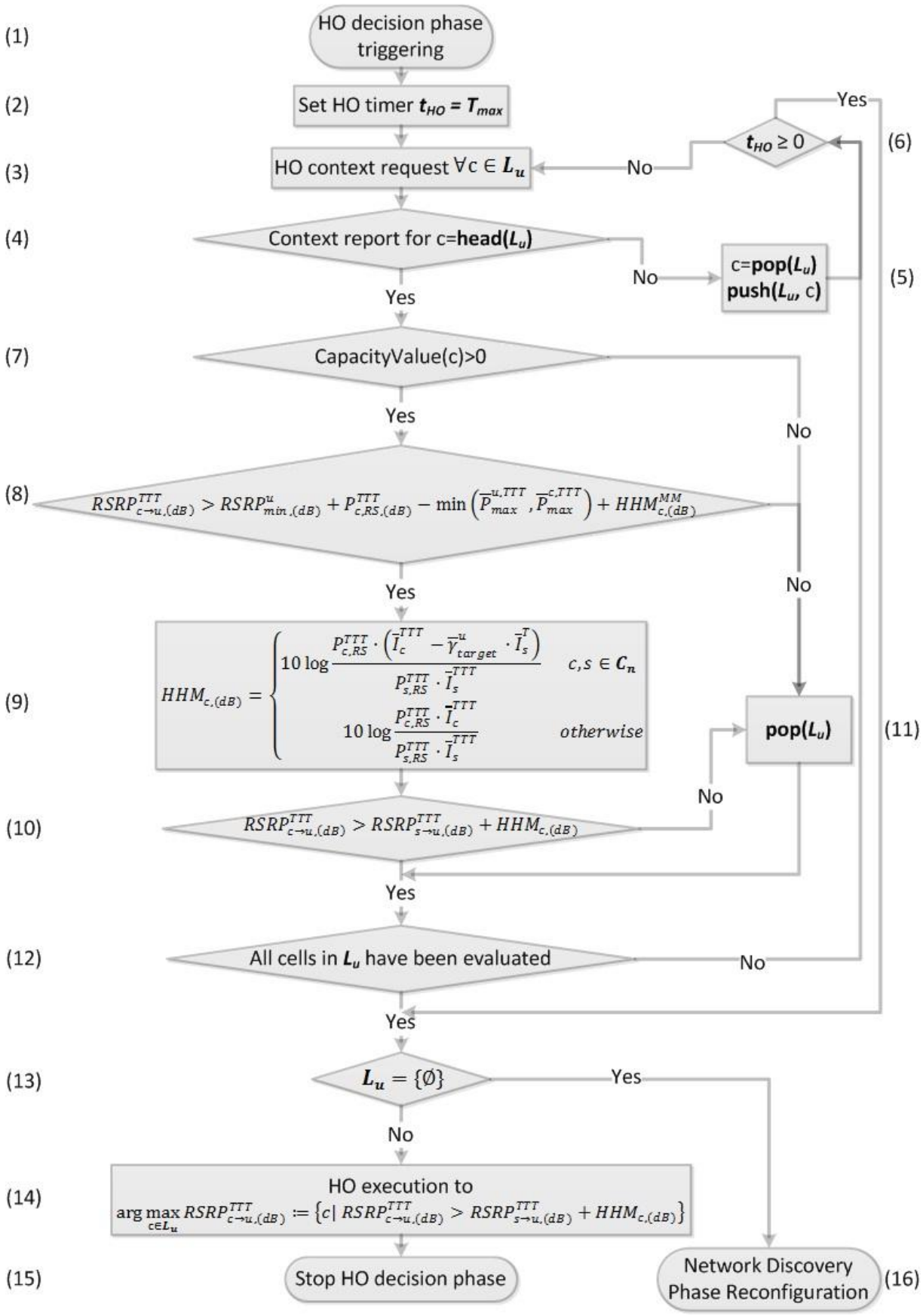

Figure 2: Proposed HO decision algorithm for the two-tier LTE-Advanced network

The proposed HO decision algorithm for the LTE-A network is illustrated in Fig. 2. Upon HO decision triggering (step 1), the proposed algorithm initializes a HO decision countdown timer, denoted by t_{HO}, to the prescribed HO decision time horizon T_{max} (step 2). This timer is assumed to be adapted with respect to critical LTE-A events, such as the ones described in [39].

In step 3, the proposed algorithm initiates a HO context acquisition request to derive the HO context describing the candidate cells' status. The network signaling procedure for performing this step is thoroughly investigated in Section 5. In step 4, the proposed algorithm handles the candidate cell set $\boldsymbol{L_u}$ as a queue structure and examines whether the required HO context for the queue head is reported to the serving cell, or not. If not, the proposed algorithm postpones the evaluation of the queue head in $\boldsymbol{L_u}$ (step 5), i.e., the queue head is moved to the end of the queue, and evaluates whether the HO decision countdown timer has expired (step 6). On the other hand, if the HO context is available to the serving cell, the proposed algorithm evaluates whether the residual capacity of the candidate cell c can support the tagged user (step 7). If not, the candidate cell c is removed from the queue structure $\boldsymbol{L_u}$ (step 11), and the evaluation procedure continues. If the residual capacity of cell c enables the support of the tagged user, the proposed algorithm evaluates whether the candidate cell c can sustain wireless connectivity (step 8). Note that this step employs the methodology for sustained wireless connectivity in Section 4.1 with the addition of a HHM, denoted by $HHM_{c,(dB)}^{MM}$, which is introduced to further lower the HO probability for medium to high speed users. The impact of the $HHM_{c,(dB)}^{MM}$ parameter on the performance of the algorithm is investigated in Section 5.

Once again, if the conditions for sustained wireless connectivity are not met, the proposed algorithm removes the candidate cell c from the queue (step 11), and proceeds with the evaluation procedure. If the condition in step (8) is met, however, the adaptive HHM for reduced UE transmit power is calculated in step (9). Accordingly, the HO decision criterion for reduced interference and energy consumption is employed (step 10), where a negative assessment leads to the removal of the candidate cell from the candidate cell set (step 11). If the HO decision criterion is met, the proposed algorithm checks whether all the candidate cells have been evaluated (step 12), and if not, the HO countdown timer is examined (step 6) and the loop in steps 3 to 12 is revisited. The proposed algorithm terminates this loop either when all the candidate cells have been evaluated (step 12), or when the HO countdown timer has expired (step 6). If at least one of these two stopping conditions is met, the proposed algorithm evaluates whether there exist candidate cells that meet the previous criteria (step 13). If such cells exist, the proposed algorithm initiates a HO to the candidate cell with the minimum required mean UE transmit power (step 14), and terminates the HO decision phase (step 15). In the opposite case, the proposed algorithm initiates a network discovery phase reconfiguration (step 16).

5. HO SIGNALING CONSIDERATIONS

This section presents the feasible HO execution scenarios for the two-tier LTE-A network and describes two different network signaling approaches for employing the proposed algorithm, depending on whether the required HO context is reported and maintained in a network entity, or not. The first signaling approach, referred to as the reactive approach, is based on acquiring the HO context on demand to the candidate cells. The second signaling approach, referred to as the proactive approach, is based on acquiring the HO context on demand to the network entity which is responsible for maintaining and disseminating this context to the LTE-A cells. This HO context management entity can be either an LTE-A core network (CN) entity, e.g., the Mobility Management Entity (MME) [1], or a peripheral entity such as the Access Network Discovery and Selection Function (ANDSF) [40]. Without loss of generality, in the following it is assumed that the MME plays the role of the HO context management entity for the proactive approach.

Different from LTE Rel. 8/9, the LTE-A standard supports direct communication between the HeNBs through the standard X2 interface [38]. X2-based HO execution between HeNBs, however, is

allowed only if no access control at the MME is needed, i.e., either when the HO is performed between closed/hybrid access HeNBs with the same CSG ID, or when the target HeNB supports open access. Even though the X2 interface is supported both between eNBs and between HeNBs, the LTE-A standard does not provision for direct X2-based communication between eNBs and HeNBs, due to the increased complexity required [31]. As a consequence, the HO execution between a) eNBs and HeNBs, or b) closed/hybrid HeNBs with different CSG IDs, or c) open access HeNBs, can only be employed through the MME and the standard S1-interface [41]. Table II summarizes the feasible HO execution scenarios for the two-tier LTE-A network and indicates the interface under use, depending on whether access control is required on the target cell, or not. Note that access control does not apply in the HO execution scenarios 1 and 2, i.e., when the target cell is an eNB, and that the serving cell in the HO scenario 3 can be either an eNB, or HeNB. The proposed HO decision algorithm applies to all the HO execution scenarios in Table II. To this end, the remainder of this section discusses the signaling procedures required for employing it, under both the reactive and the proactive HO context acquisition approaches.

Table II: HO execution scenarios in the two-tier LTE-A network

HO Scenario	Serving Cell	Target Cell	Access Control	HO Type	HO Execution Interface
1	eNB	eNB	Does not apply	Regular E-UTRAN	X2
2	HeNB	eNB	Does not apply	Outbound from HeNB	S1
3	(H)eNB	HeNB	Yes	Inbound to HeNB	S1
4	eNB	HeNB	No	Inbound to HeNB	S1
5	HeNB	HeNB	No	Inbound to HeNB	X2 / S1

Fig. 3 illustrates the signaling procedure for the HO scenario 1 under the reactive HO context acquisition approach. Steps 0 – 2 correspond to the cell search and measurement phase at the UE. The HO decision algorithm is triggered in step 3, where the serving eNB signals a HO context request towards the candidate eNB through the X2-interface (step 4). Upon reception of the HO context report (step 5), the serving eNB reaches to a HO decision (step 6), and initiates the standard HO execution procedure (steps 7 – 21) [1]. Different from the reactive approach, the proactive approach (Fig. 4) includes a periodic MME-configured HO context acquisition phase (steps 1 – 2) prior to the HO decision phase (steps 7 – 9). The HO context request/report signals in steps 7 – 8 are initiated towards the MME through the S1 interface, rather than the target eNB through the X2 interface. Note that both the network discovery and the HO execution phases, i.e., steps 3 – 5 and steps 10 – 24, respectively, follow the standard signaling procedure as in the reactive approach (Fig. 3). Both the reactive and proactive signaling approaches for the HO execution scenario 2, i.e., HO from a HeNB to an eNB, are similar to the ones followed in Fig. 3 and 4, respectively, and they are omitted due to space limitations. The key difference between the HO execution scenarios 1 and 2 is that the signaling procedure between the serving HeNB and the target eNB is performed through the MME and the S1 interface, i.e., steps 4, 5, 7, 9, and 11 in Fig. 3, and steps 10, 12, 14 in Fig. 4, given that the LTE-A standard does not support X2-based communication between HeNBs and eNBs.

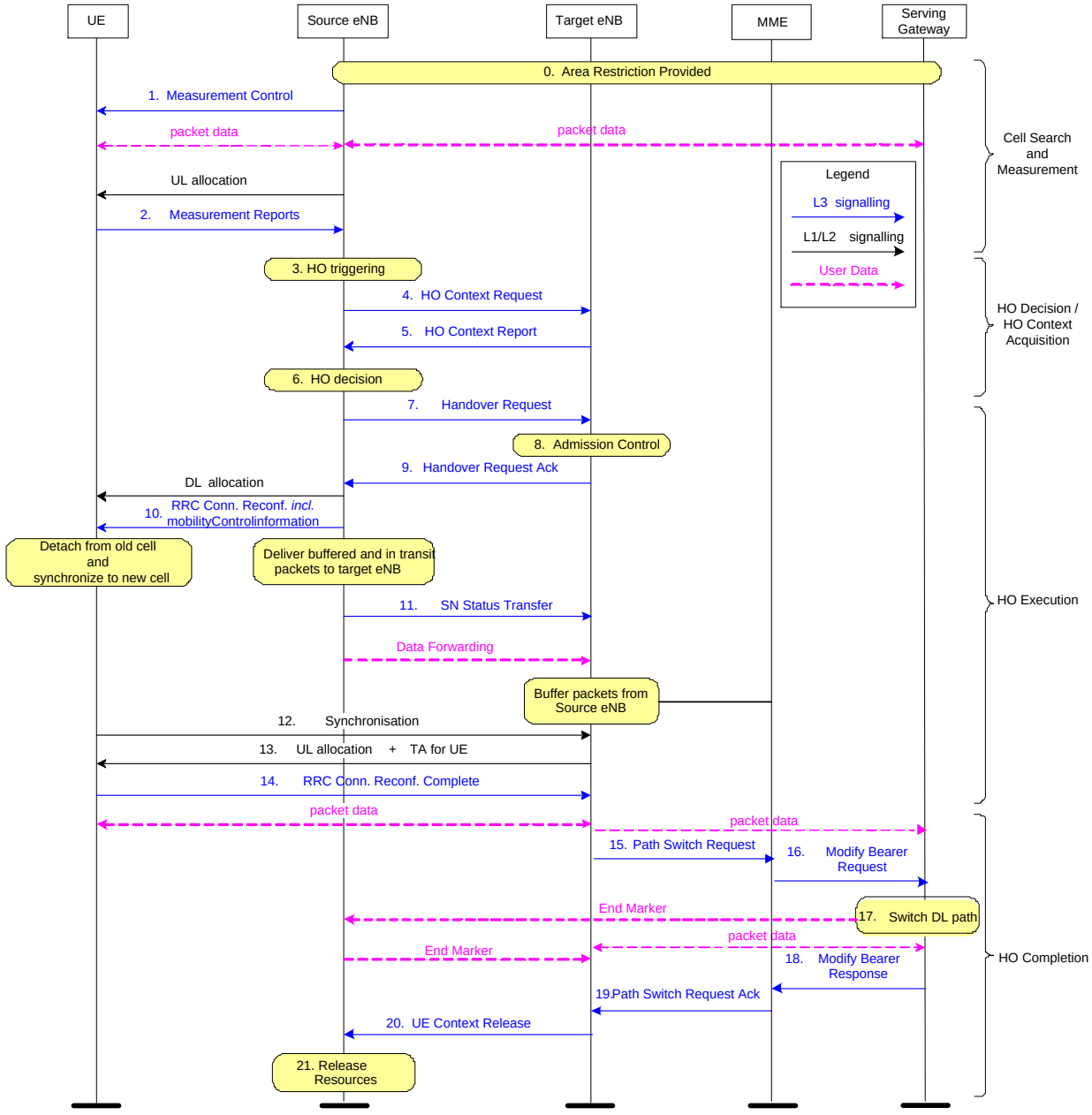

Figure 3: Reactive HO context acquisition approach for the HO execution scenario 1

Let us now focus on the HO signaling procedure for supporting inbound mobility towards a HeNB. Fig. 5 illustrates the reactive HO signaling procedure for the HO execution scenario 3, i.e., eNB-to-HeNB, or HeNB-to-HeNB with access control. Note that the deployment of the HeNB Gateway is optional [1].

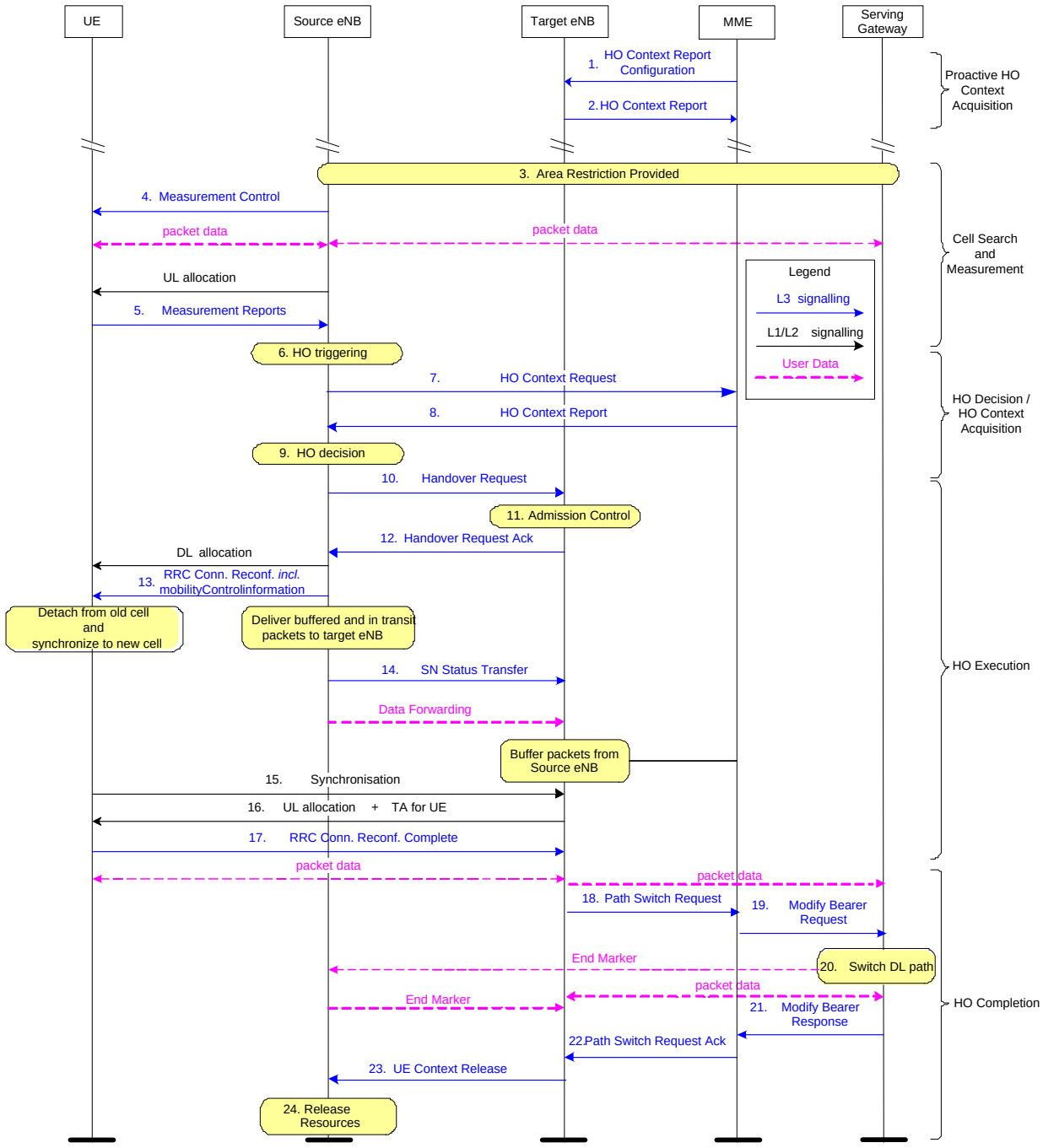

Figure 4: Proactive HO context acquisition approach for the HO execution scenario 1

The cell search and measurement phase is performed in steps 1 – 7, and consists of the proximity indication (steps 1 – 2), measurement derivation (step 3 – 4), and cell identification (steps 5 – 7) phases [1]. Upon HO decision triggering (step 8), the serving (H)eNB initiates a HO context request towards the target HeNB through the S1 interface (steps 9 – 11), i.e., via the MME and the HeNB-GW. The target HeNB reports the required HO context (steps 12 – 14), and the HO decision algorithm terminates in step (15). Note that when the serving cell is a HeNB, the HO context request/report signals can be exchanged through the X2 interface. The HO procedure is completed in steps 16 – 24, where the standard HO execution phase takes place through the S1 interface. It should be noted that the HO execution phase is performed through the S1 interface regardless the type of the serving eNB, i.e., eNB or HeNB, given that MME-based access control is required for the HO execution scenario 3 (step 17). The key difference between the reactive and the proactive HO context acquisition

approaches in the HO execution scenario 3, i.e., Fig. 5 and 6, respectively, is that in the proactive one the serving eNB acquires the HO context on demand to the MME (steps 13 – 14), which configures the target HeNB to report the HO context on a periodic basis (steps 1 – 4).

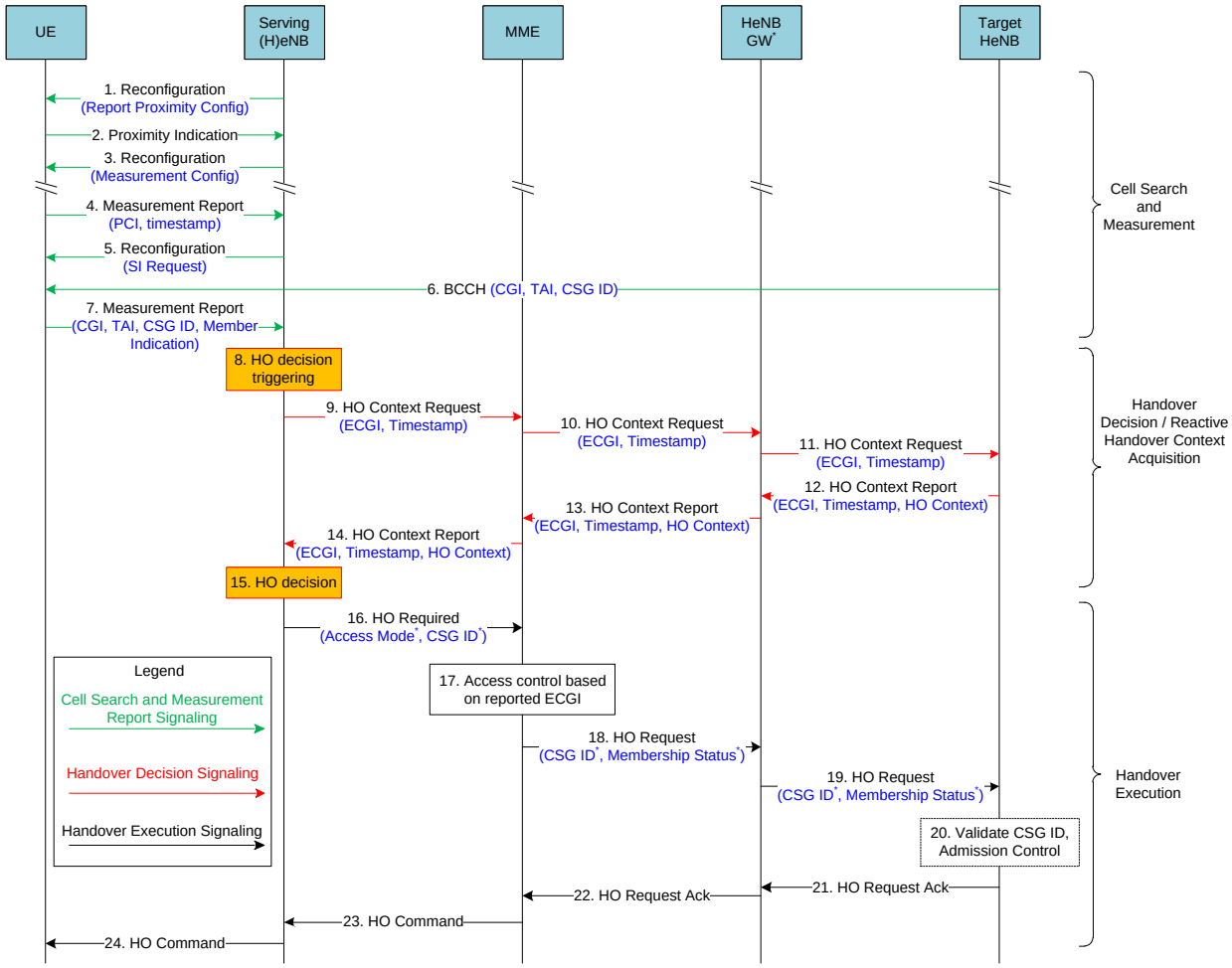

Figure 5: Reactive HO context acquisition approach for the HO execution scenario 3

Both the reactive and the proactive signaling approaches for the HO execution scenario 4 are similar to the ones depicted in Fig. 5 and 6, respectively, with the difference that the MME-based access control step is omitted (step 17). The same implies for the HO execution scenario 5, where in addition, the serving and the target HeNB can utilize the standard X2 interface to perform both the HO execution phase (steps 16 – 23 in Fig. 5 and 6), and the HO context acquisition phase for the reactive signaling approach (steps 9 – 14 in Fig. 5).

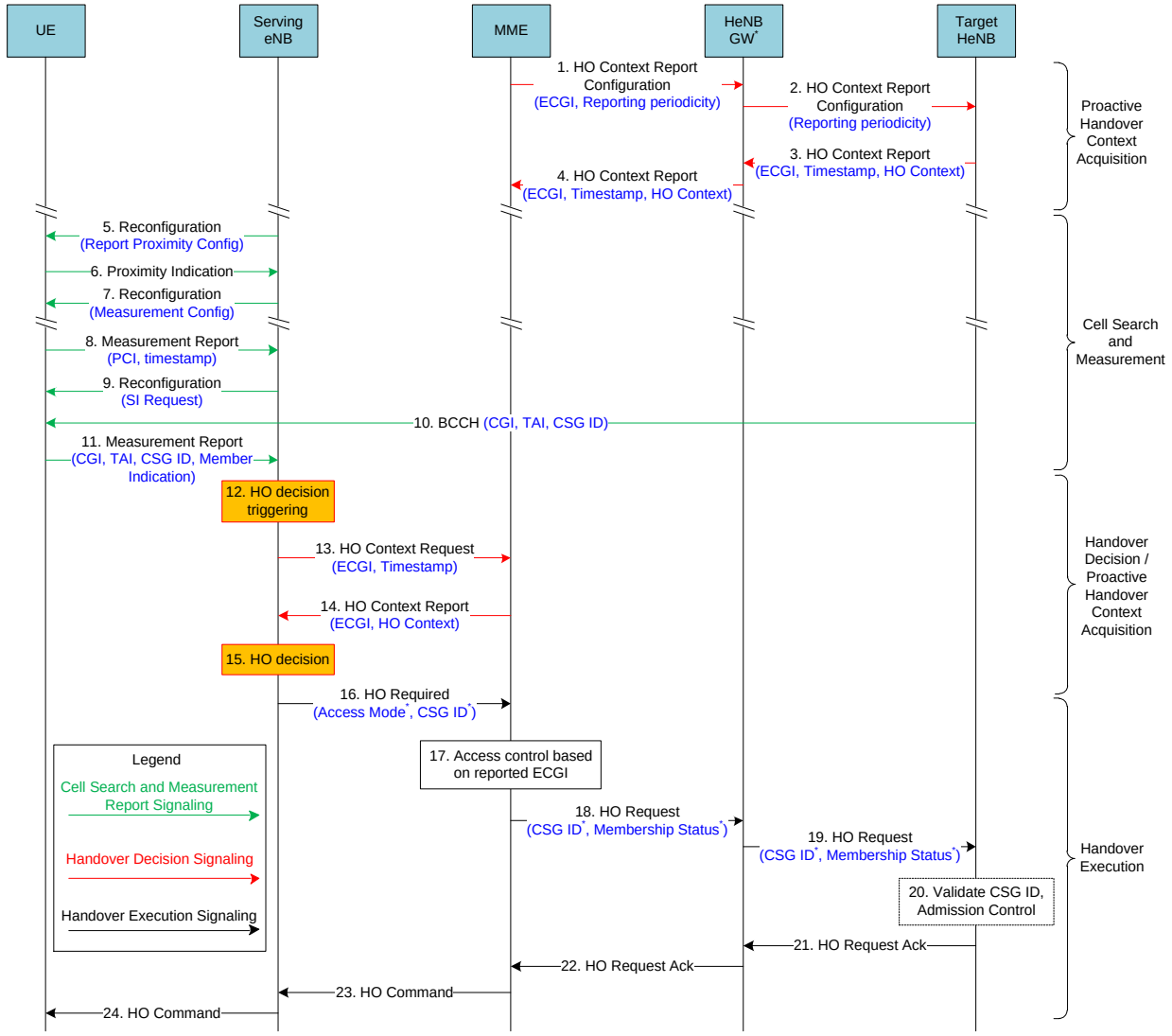

Figure 6: Proactive HO context acquisition approach for the HO execution scenario 3

Let us now focus on how the HO context request/report signals can be performed. The LTE-A standard describes a wide set of signals for the S1 and the X2 interfaces which, however, are not provisioned to transfer the entire HO decision context required for employing the proposed algorithm. Nevertheless, the HO context acquisition signaling can be performed either a) by using the private message mechanism for non-standard use described in [38] for the X2 interface, and in [41] for the S1 interface, or b) by introducing a new message type in future amendments of the LTE-A standard, to include the entire HO decision context required. The use of the private mechanism for non-standard use is already part of the LTE-A standard, and thus, the proposed HO decision algorithm can be employed with a simple software update at the eNBs, HeNBs, and the MME. On the other hand, the addition of a new message type and Information Element (IE) containing the required HO context, will enhance the functionality of the LTE-A system towards more sophisticated mobility and interference management support.

Referring to the differences of the reactive and proactive HO context acquisition approaches, the reactive approach is expected to lower the HO context request/report signaling commuted through the LTE-A CN, especially when an X2 interface is established between the serving and the target cells. On the other hand, the proactive approach is expected to minimize the signaling overhead towards the LTE-A cells, as it eliminates the occurrence of multiple HO context report/ request signals for the

same HO context. More frequent yet deterministic signaling overhead is expected for the proactive approach where the HO context signaling periodicity is configured by the MME, compared to the reactive approach, where the consequential signaling overhead is highly correlated to the occurrence rate of the HO events. Nevertheless, the proactive approach necessitates enhanced HO context management functionality at the LTE-A CN, in contrast with the reactive approach where no additional functionality enhancements are required.

6. NUMERICAL RESULTS

This section includes extensive system-level simulation results to demonstrate the performance of the proposed MM approach. Section 6.1 summarizes the adopted simulation model and parameters, whereas Section 6.2 presents selected numerical results.

6.1 System-level simulation model and parameters

This section investigates the performance of the proposed mobility management approach, under both HO context acquisition procedures, based on an extended version of the system-level evaluation methodology described in [8]. A hexagonal LTE-A network is considered with a main cluster composed of 7 eNBs, where each eNB consists of 3 sectors. The wrap-around technique is used to extend the LTE-A network, by copying the main cluster symmetrically on each of the 6 sides. A set of blocks of apartments, referred to as femtoblocks, are uniformly dropped within the main cluster area with respect to the femtoblock deployment density parameter, denoted by d_{FB}, which indicates the percentage of the main cluster area covered with femtoblocks. Femtoblocks are modeled according to the dual stripe model for dense urban environments in [8], where each femtoblock consists of two stripes of apartments separated by a 10 m wide street and each stripe has two rows of 5 apartments of size 10x10m. The deployment of femtocells within each femtoblock is based on the femtocell deployment ratio parameter, denoted by r_{fc}, which indicates the percentage of femtoblock apartments with a femtocell installed. Femtocell stations and users are uniformly dropped inside the apartments, where each femtocell station initially serves one user. Each macrocell sector initially serves ten users, which are uniformly distributed within it. The LTE-A users are members of up to one CSG, where three CSG IDs are used in the network. The remainder simulation parameters are summarized in Table III.

Note that a higher d_{FB} corresponds to a denser femtoblock layout within the main LTE-A cluster, while a higher r_{fc} to a denser femtocell deployment within the femtoblocks. As a result, although a higher d_{FB} or r_{fc} parameter results in denser femtocell deployment layout, a higher r_{fc} leads to comparably denser femtocell deployment within small areas, i.e., femtoblock. It should also be noted that a higher d_{FB} or r_{fc} parameter results in the introduction of additional UEs in the network, provided that each femtocell is assumed to initially serve one user. The performance of the proposed approach is evaluated under both the HO context acquisition approaches, where the reactive version of the algorithm is referred to as Prop-R and the proactive as Prop-P3s. Different performance is attained for the two different versions of the proposed algorithm, given that the HO context update for the Prop-P3s algorithm is performed once every 3 seconds. The Prop-R and Prop-P3s are compared against the SC HO decision algorithm, referred to as the SC algorithm, and the algorithm in [31], referred to as the Zhang11 algorithm.

Table III: System-level simulation model and parameters

Network layout			
Macrocell layout			7 clusters, 7 sites per cluster, 3 sectors per site, freq. reuse 1
Macrocell inter-site distance			500 m
Initial number of UEs per macrocell sector			10 UEs
Macrocell UE distribution			Uniform within each sector
Femtoblock layout			Dual stripe model for dense urban environments [8]
Femtoblock distribution in the main LTE-A cluster			Uniform
Femtocell station and UE distribution within an apartment			Uniform
Initial number of UEs per femtocell station			1 UE
Maximum number of supported UE per femtocell			4 UEs
System operating parameters			
Parameter	**Macrocell**		**Femtocell**
Carrier frequency	2000 MHz		Uniformly picked from the set {1990, 2000, 2010} MHz
Channel bandwidth	10 MHz		10 MHz
Maximum Tx Power	$\overline{P}_{max}^{c,T} = 46$ dBm		$\overline{P}_{max}^{c,T} = 20$ dBm
Antenna gain	14 dBi		0 dBi
Noise figure	5 dB		8 dB
Shadowing standard deviation	8 dB		4 dB
RS transmit power (DL RS Tx)	Normally distributed with a mean value of 23 dBm and standard deviation 3dB		Uniformly distributed within the [0,20] dBm interval
CSG ID distribution	Does not apply		Uniform within {1, 2, 3}
Link-to-system mapping	Effective SINR mapping (ESM) [8]		
Path Loss Models			
Path loss			Models for urban deployment in [8]
Interior / Exterior wall penetration loss (indoor UEs)			5 / 15 dB
UE parameters			
UE power class	$\overline{P}_{max}^{u,T} = 23$ dBm		
UE antenna gain	0 dBi		
Mean UL SINR target	$\overline{\gamma}_{target}^{u} = 3$ dB		
CSG ID distribution	Uniformly picked from {1, 2, 3}		
Traffic model	Full buffer similar to [8]		
Mobility model [13]	User speed	$v_t = N(\bar{v}, s_u)$ m/s	
		Mean user speed	$\bar{v} = 3$ km/h
		User speed standard deviation	$s_u = 1$ km/h
	User direction	$\varphi_t = N\left(\varphi_{t-1}, 2\pi - \varphi_{t-1}\tan\left(\frac{\sqrt{v_t}}{2}\right)\Delta t\right)$	
	where Δt is the time period between two updates of the model, and $N(a, b)$ the Gaussian distribution of mean a and standard deviation b		
Other simulation parameters			

Overall simulation time	200 sec
Simulation time unit	$\Delta t = 1$ sec
HO context updating periodicity for the Prop-P3s algorithm	3 sec

6.2 System-level simulation results

Fig. 7 illustrates the performance of the algorithms in terms of mean UE transmit power for varying femtoblock deployment density d_{FB}. Two different femtocell deployment ratios r_{fc} are used to investigate the algorithms' performance under both sparse and dense femtocell deployments per femtoblock, i.e., $r_{fc} = 0.1$ and $r_{fc} = 0.5$, respectively.

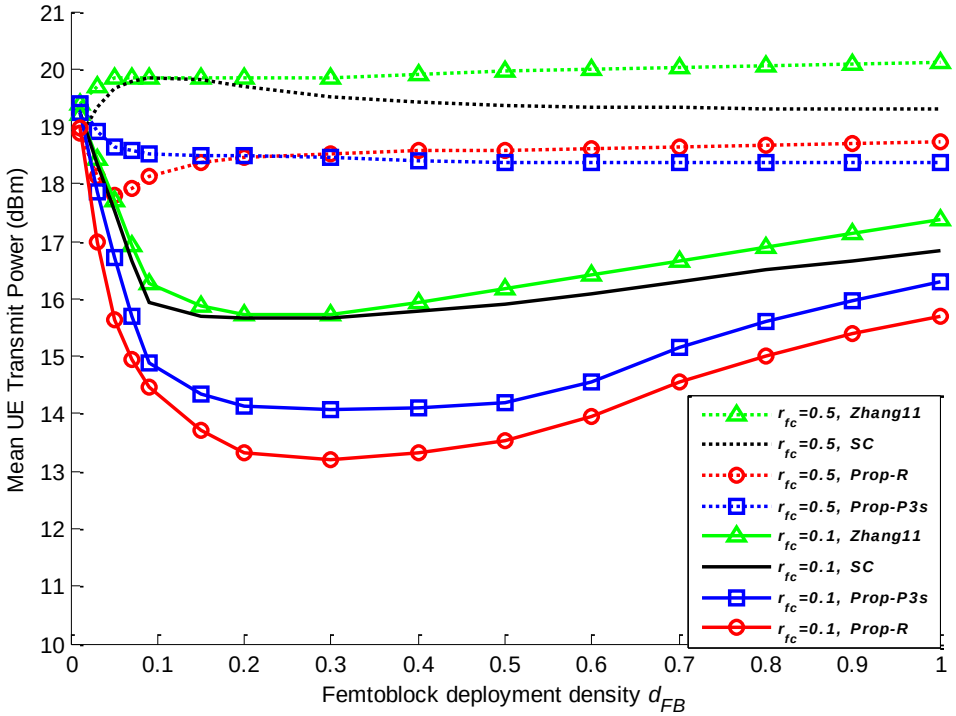

Figure 7: Mean UE transmit power vs. the femtoblock deployment density

For $r_{fc} = 0.1$, the mean UE transmit power lowers for all algorithms as the d_{FB} increases, owing to the shorter transmit – receive range of the sparsely deployed femtocell infrastructure. Above a certain d_{FB}, however, higher mean UE transmit power is required to sustain the mean UL SINR target $\overline{\gamma}^{u}_{target}$ for all algorithms, due to the comparably shorter inter-site distance between the HeNBs which rapidly raises the interference at the cell sites (Fig. 8). Depending on the femtoblock deployment density d_{FB}, the Prop-R algorithm is shown to lower the mean UE transmit power from 0.5 to 2.6dB compared to the SC and the Zhang11 algorithms, i.e., 11% to 45% gain. Improved performance is attained by the Prop-P3s algorithm as well, where the respective gain is shown to reach up to 1.7 dB, i.e., 33%. Higher mean UE transmit power is required for all algorithms in denser femtocell deployments per femtoblock ($r_{fc} = 0.5$), where comparably shorter mean inter-site distance characterizes the femtocell layout even under low femtoblock deployment densities ($d_{FB} < 0.1$). Different from the competing algorithms, the Prop-R and Prop-P3s algorithms improve their performance for low d_{FB} values, while increased yet almost constant transmit power is observed for all algorithms in medium to high d_{FB} values. Once again, both versions of the proposed algorithm are shown to require up to 2dB lower UE transmit power compared to the competing algorithms, i.e., 37% gain, as they account for the actual interference level at the cell sites and the channel gain between the UEs and the (H)eNBs.

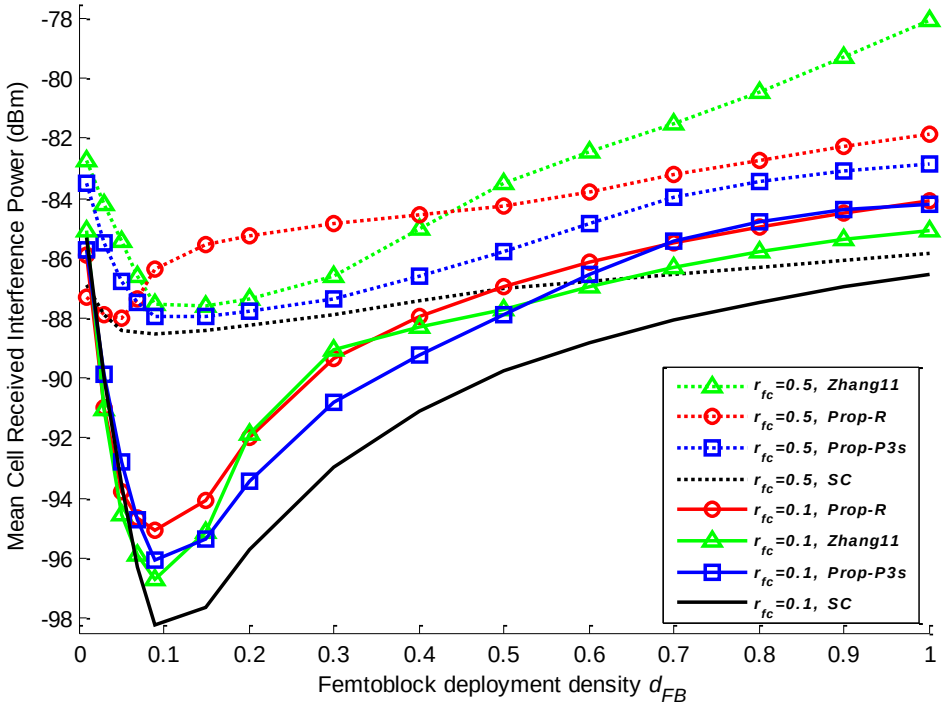

Figure 8: Mean cell received interference power vs. the femtoblock deployment density

Fig. 8 depicts the performance of the algorithms in terms of mean received interference power at the cell sites, for varying d_{FB} and two r_{fc} values. As expected, a denser femtocell deployment per femtoblock ($r_{fc} = 0.5$) raises the interference at the cell sites for all algorithms, owing the short inter-site distance between the HeNBs. For $r_{fc} = 0.1$ on the other hand, even though a sparser femtoblock layout reduces the mean interference at the cell sites ($d_{FB} \leq 0.1$), above a d_{FB} value the mean interference level rapidly increases for all algorithms. The SC algorithm attains lower interference compared to the femtocell-specific algorithms, while compared to the Prop-R and the Zhang11 algorithms, improved performance is shown for the Prop-P3s algorithm as well. Interestingly, even though the Prop-R algorithm greatly lowers the mean UE transmit power compared to the other algorithms (Fig. 7), it simultaneously results in higher cell interference under the same network layouts (Fig. 8). This result follows from the comparably enhanced femtocell utilization attained by the Prop-R algorithm, which substantially raises the number of femtocell users compared to the competing algorithms (Table IV).

Table IV: Number of femtocell users / total number of users within the main LTE-A cluster

d_{FB}	**Number of femtocell users / total number of users**							
	$r_{fc} = 0.1$				$r_{fc} = 0.5$			
	SC	**Zhang11**	**Prop-P3s**	**Prop-R**	**SC**	**Zhang11**	**Prop-P3s**	**Prop-R**
0,01	2,5/211	3/211	8/211	8/211	7,5/218	7,5/218	10,5/218	10/218
0,05	7,5/215	7/215	22/215	29/215	14/242	14/242	27,5/242	29/242
0,1	17,5/224	16,5/224	42/224	52,5/224	19,5/271	17/271	36,5/271	53,5/271
0,25	27/239	29/239	66,5/239	75,5/239	39,5/359	55,5/359	62/359	74/359
0,5	45,5/269	56,5/269	88/269	105/269	77,5/500	99/500	107/500	129,5/500

0,75	52/303	69,5/303	109,5/303	128,5/303	115,5/641	142,5/641	158/641	193,5/641
1	60,5/337	82,5/337	136/337	159/337	153,5/782	186/782	209/782	257,5/782

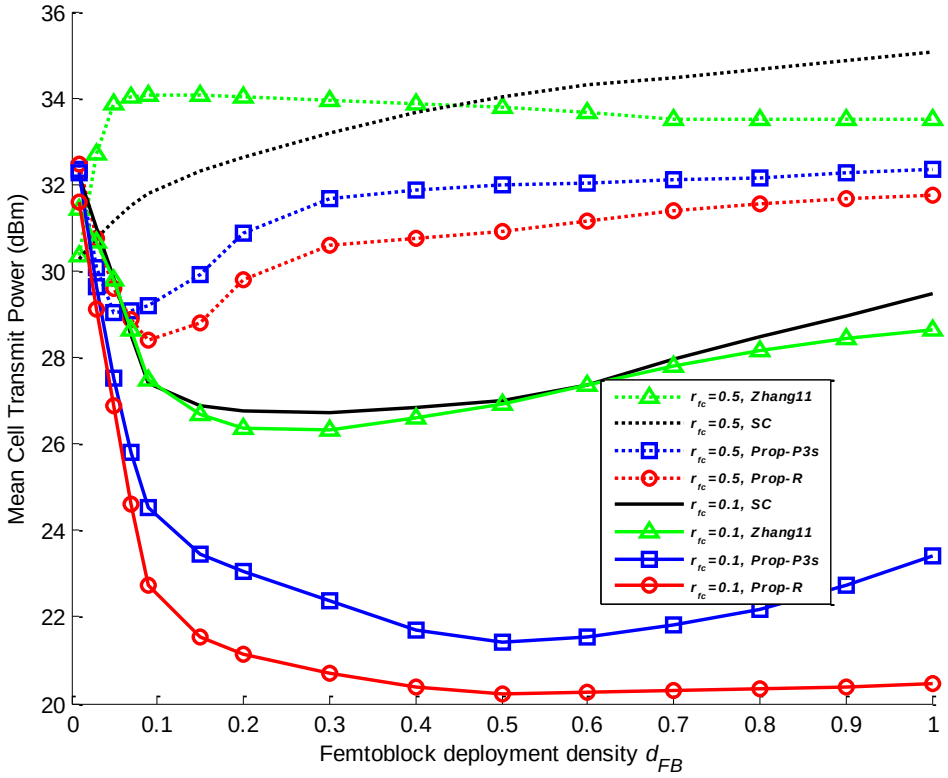

Figure 9: Mean cell transmit power vs. the femtoblock deployment density

Fig. 9 depicts the mean cell transmit power performance of all algorithms, for varying d_{FB} and two different r_{fc} values. Note that for dense femtocell deployment per femtoblock ($r_{fc} = 0.5$) and low d_{FB} values, the Zhang11 algorithm increases the mean cell transmit power as it prioritizes femtocell access regardless the interference and propagation conditions at the UEs and the femtocell sites. For higher d_{FB} values, however, the performance of the algorithm improves due to the shorter femtocell inter-site distance. The Prop-R and Prop-P3s algorithms are shown to substantially lower the mean cell transmit power compared to the SC and Zhang11 algorithms, with the higher gains attained for sparse femtocell deployment ratios ($r_{fc} = 0.1$) and medium to high femtoblock deployment densities, i.e., up to 9 dB gain for the Prop-R and 6dB for the Prop-P3s algorithm.

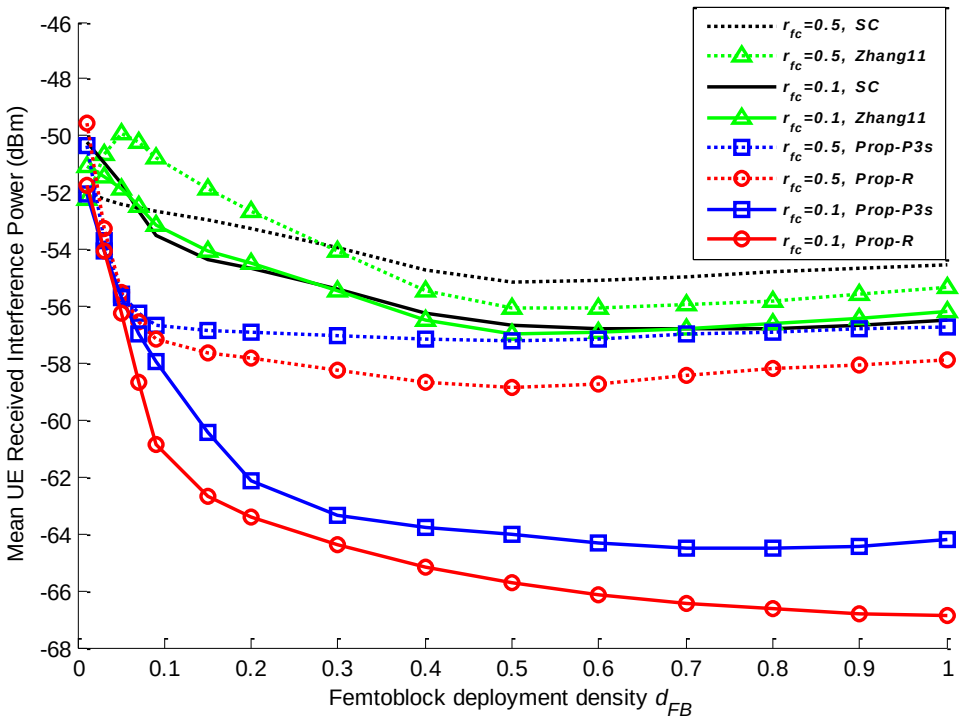

Figure 10: Mean UE received interference power vs. the femtoblock deployment density

The greatly lower mean cell transmit power attained by both the Prop-R and Prop-P3s algorithms, results in significantly reduced interference at the UEs as well (Fig. 10). Noticeably, the performance of the Prop-R and Prop-P3s algorithms under dense femtocell deployment per femtoblock is better even compared to the one of the competing algorithms in sparse femtocell deployments per femtoblock. For $r_{fc} = 0.1$ the SC and Zhang11 algorithms show similar performance, whereas the Prop-R and Prop-P3s algorithms are shown to lower the mean UE interference by up to 10 and 8dB, respectively. Significantly lower mean UE interference is shown for the Prop-R and Prop-P3s algorithms under $r_{fc} = 0.5$ as well, with the higher gains attained under low to medium femtoblock deployment densities, i.e., $0.05 < d_{FB} < 0.3$. Note that the UE interference mitigation plays a key role for realizing the femtocell communication paradigm, given that the employment of interference management and self-optimization is typically performed at the LTE-A network rather than the UE side.

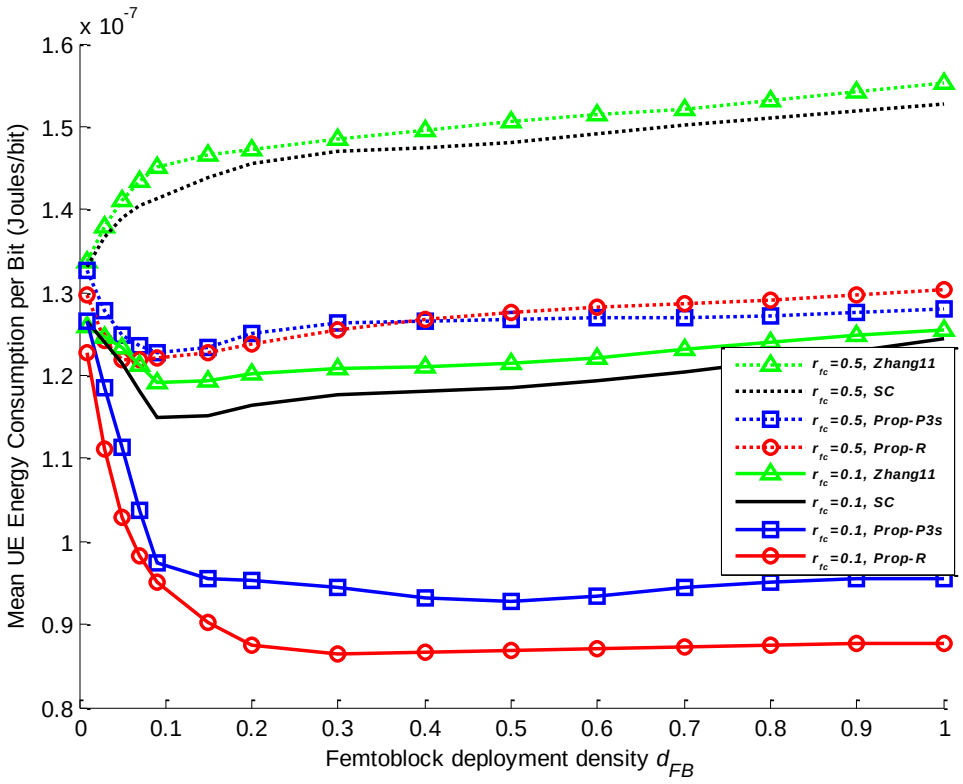

Figure 11: Mean UE energy consumption per bit vs. the femtoblock deployment density

Fig. 11 illustrates the performance of the algorithms in terms of mean UE energy consumption per bit, owing to transmit power. For dense femtocell deployment per femtoblock ($r_{fc} = 0.5$), as the d_{FB} increases constantly increasing UE energy expenditure per bit is required for the SC and Zhang11 algorithms to sustain the mean UL SINR target $\overline{\gamma}^{u}_{target}$. On the other hand, improved performance is achieved for the Prop-R and Prop-P3s algorithms as the d_{FB} increases, where for $d_{FB} > 0.1$ rising yet comparably lower energy consumption per bit is required as well, compared to the competing algorithms. For sparse femtocell deployments per femtoblock ($r_{fc} = 0.1$), reduced energy expenditure overhead per bit is observed for all algorithms. Both versions of the proposed algorithm, however, attain substantially enhanced UE energy expenditure per bit compared to the competing algorithms, even for very low femtoblock deployment densities ($d_{FB} \geq 0.05$). Noticeably, the performance of all algorithms remains roughly unaffected above a certain d_{FB} value, i.e., $d_{FB} > 0.3$. Apart from enhanced UE energy consumption per bit, both versions of the proposed algorithm are shown resourcefully utilize the enhanced capacity potential offered by the femtocell infrastructure as well (Fig. 12).

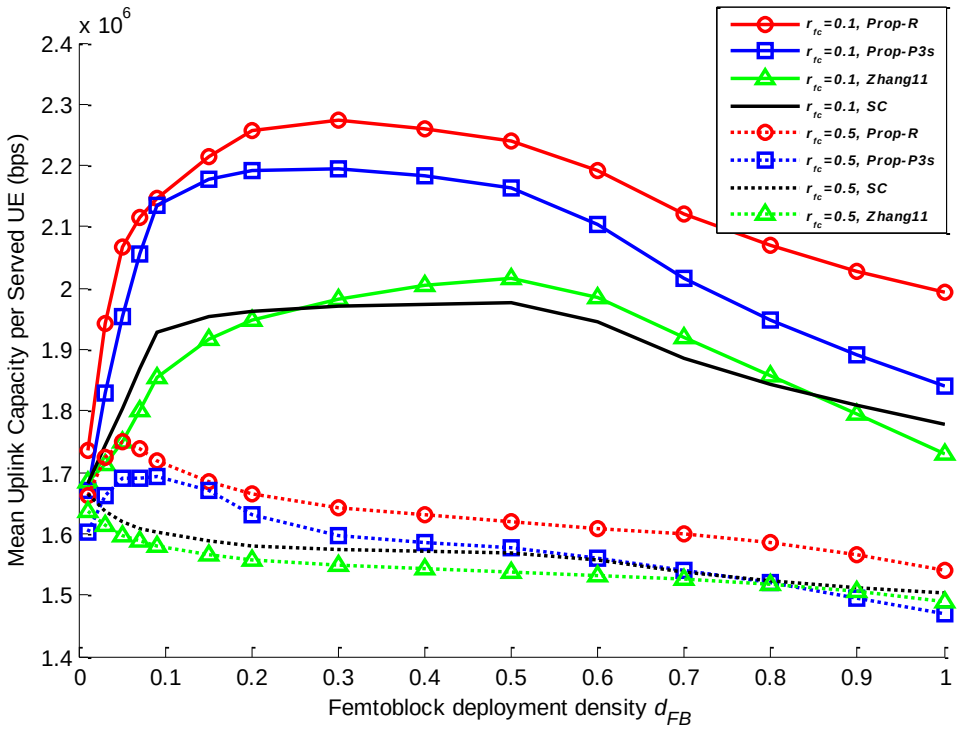

Figure 12: Mean uplink capacity per served user vs. the femtoblock deployment density

Compared to the SC and Zhang11 algorithms, which attain a similar behavior, the Prop-R algorithm is shown to enhance the mean UL capacity per served UE by up to 16% for $r_{fc} = 0.1$, and up to 9% for $r_{fc} = 0.5$. Lower yet comparable UL capacity gains are shown for the Prop-P3s algorithm as well, with the higher gains attained under low to medium femtoblock deployment densities. Even though a higher r_{fc} improves the overall network capacity, it simultaneously degrades the UL capacity per served UE for all algorithms (Fig. 12), owing to the comparably higher interference level at the cell sites (Fig. 8). Similar performance degradation is observed for higher d_{FB} values as well, where above a certain d_{FB} value the UL capacity per served UE degrades rather than improves depending on the HO decision algorithm and the r_{fc} value.

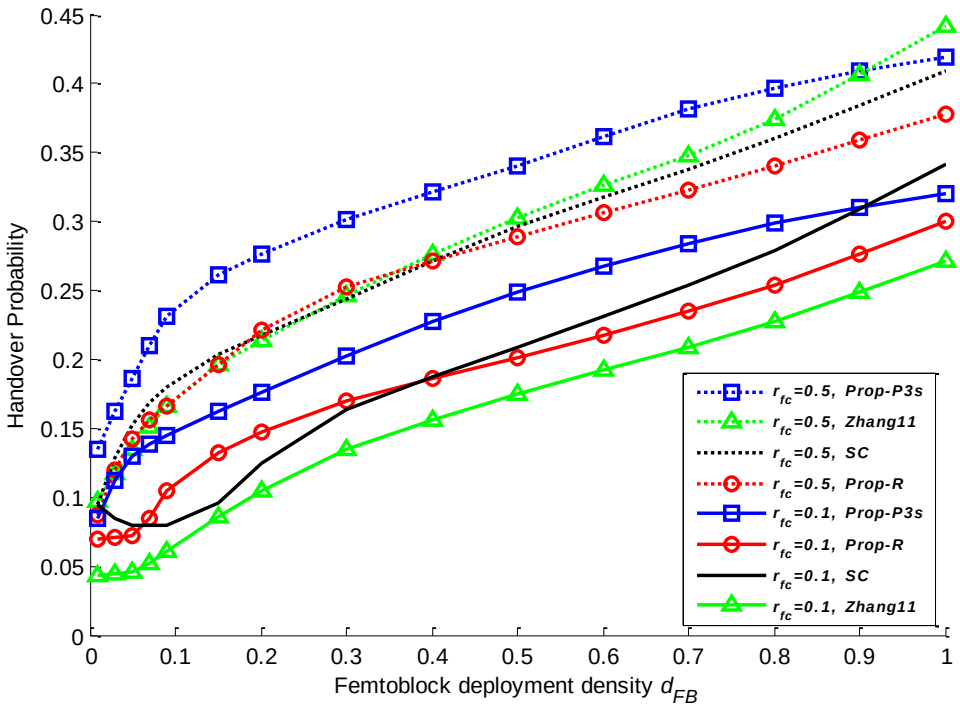

Figure 13: Handover probability vs. the femtoblock deployment density

Fig. 13 depicts the HO probability performance for all algorithms for varying d_{FB} parameter. As expected, a higher HO probability is observed for all algorithms as the d_{FB} increases. The same implies for denser femtocell deployment per femtoblock ($r_{fc} = 0.5$), where a comparably lower mean inter-site distance characterizes the femtocell deployment layout. For $r_{fc} = 0.1$ the Zhang11 algorithm is shown to sustain the lowest HO probability, whereas the Prop-R algorithm attains an improved performance compared to the SC algorithm under very low and medium to high d_{FB}, i.e., for $d_{FB} < 0.1$ and $d_{FB} \geq 0.4$, respectively. On the other hand, the Prop-P3s algorithm results in the highest HO probability for both sparse and dense femtocell deployment ratios, while for $r_{fc} = 0.5$, even though the SC, Zhang11, and Prop-R algorithms show similar performance under low to medium deployment densities ($d_{FB} < 0.4$), in medium to high femtoblock deployment densities the Prop-R algorithm attains the lowest HO probability ($d_{FB} \geq 0.4$). As will be shown in the following, the HO probability of the Prop-R and Prop-P3s algorithms can be greatly lowered by using a higher $HHM_{c,(dB)}^{MM}$ value.

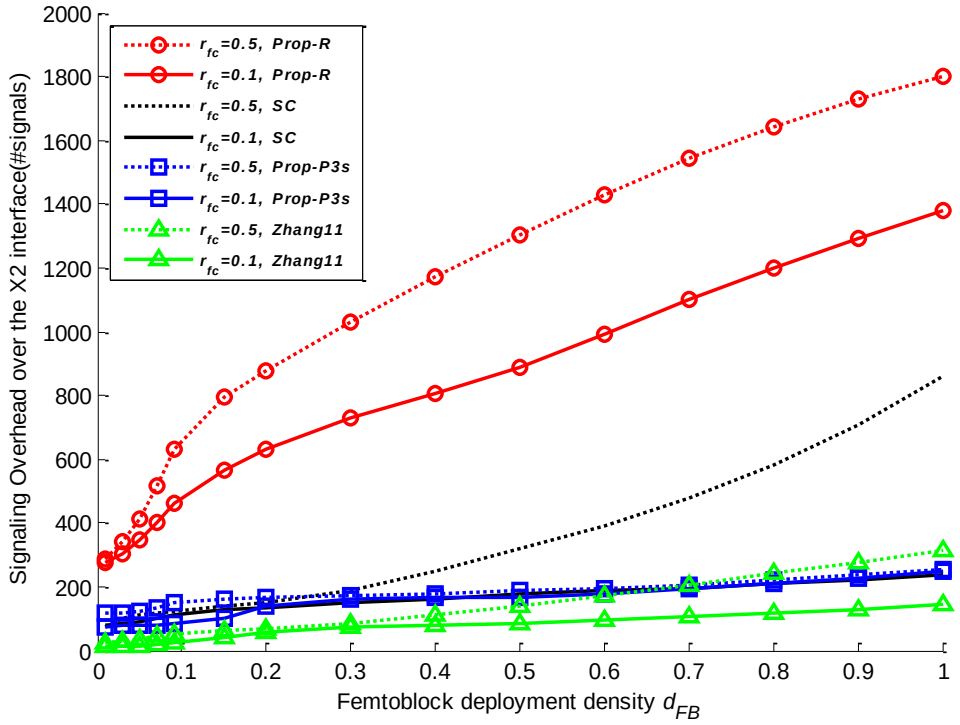

Figure 14: Signaling overhead over the X2 interface vs. the femtoblock deployment density

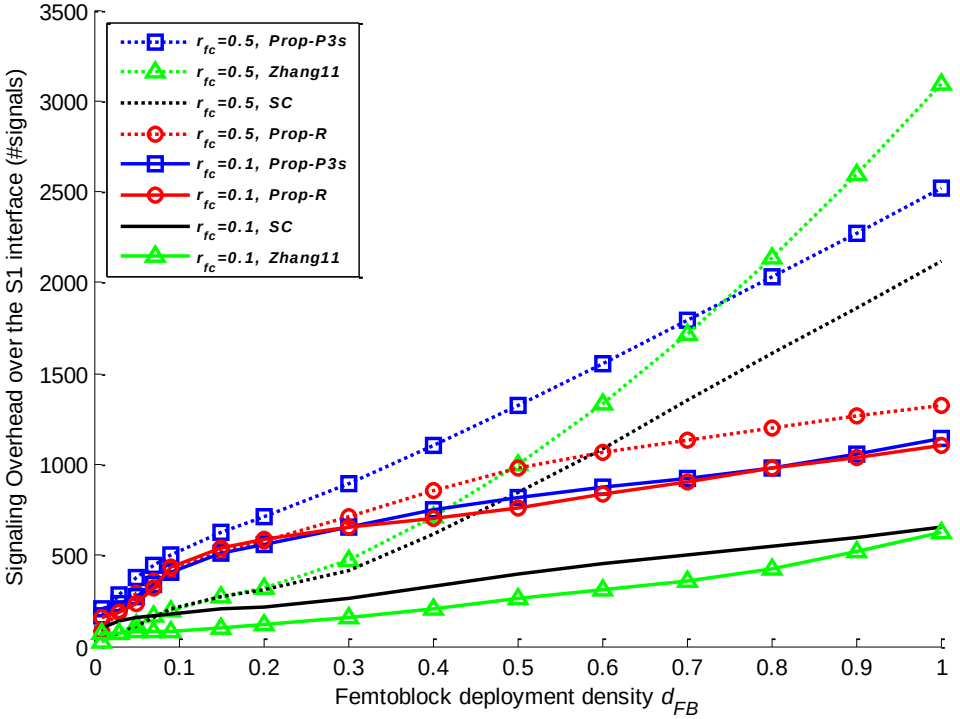

Figure 15: Signaling overhead over the S1 interface vs. the femtoblock deployment density

Fig. 14 and 15, depict the network-wide X2 and S1 signaling overhead per second, respectively, for all algorithms. Note that the depicted overhead includes both the HO execution and the HO context acquisition signaling (where necessary). In terms of X2 signaling (Fig. 14), a higher femtoblock deployment density or femtocell deployment ratio enlarges the X2 signaling overhead for all algorithms due to the denser network layout. Higher X2 signaling requirements are shown for Prop-R algorithm, under both sparse and dense femtocell deployments per femtoblock, owing to the HO

context acquisition procedure on a per candidate cell basis. Enlarged X2 signaling overhead is also observed for the SC algorithm for $r_{fc} = 0.5$, whereas the performance of the Prop-P3s algorithm is shown to remain almost unaffected due to the MME-based HO context acquisition procedure over the S1 interface.

Different from the X2 signaling, the S1 signaling performance for all algorithms is shown to be strongly affected by the femtocell deployment ratio (Fig. 15). For $r_{fc} = 0.1$ the performance of all algorithms grows almost linearly with respect to the d_{FB}. However, both versions of the proposed algorithm necessitate higher S1 signaling overhead due to the employment of the HO context acquisition. For $r_{fc} = 0.5$, a rapidly growing S1 signaling overhead is observed for the SC and the Zhang11 algorithms, whereas under medium to high d_{FB} the Prop-R algorithm is shown to require the lowest S1 signaling overhead, owing to the increased utilization of the X2 interface (Fig. 14). On the other hand, the Prop-P3s algorithm is shown to require the highest signaling overhead compared to the other algorithms, which however grows roughly linearly with respect the d_{FB} parameter. Note that the S1 signaling overhead for the Prop-P3s algorithm can be mitigated by using a lower HO context acquisition periodicity at the MME. Reduced S1 signaling is also attained for both the Prop-R and Prop-P3s algorithms if a higher $HHM_{c,(dB)}^{MM}$ is used, given that the X2 and S1 signaling strongly depend on the HO probability.

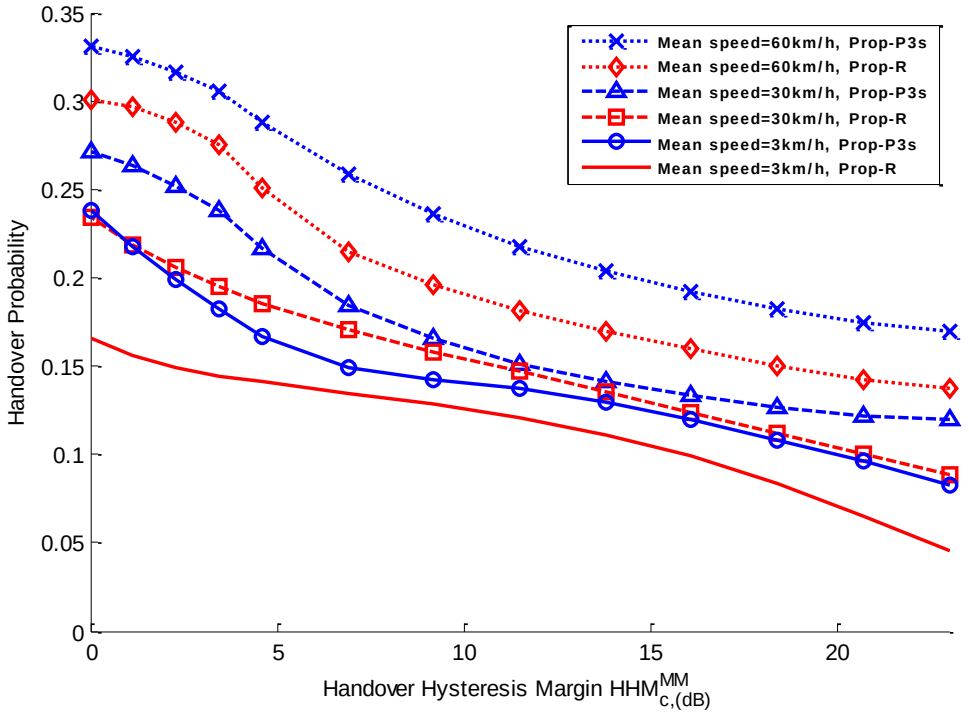

Figure 16: Handover probability vs. the Handover Hysteresis Margin $HHM_{c,(dB)}^{MM}$

Focusing on the Prop-R and Prop-P3s algorithms, Fig. 16 and 17 depict the HO probability and mean UE transmit power performance, respectively, for varying $HHM_{c,(dB)}^{MM}$ parameter and various mean user speeds. These results are derived for $d_{FB} = 0.2$ and $r_{fc} = 0.3$. As expected, a higher user speed increases the HO probability for both versions of the proposed algorithm. Nevertheless, a higher $HHM_{c,(dB)}^{MM}$ value can be used to lower the HO probability depending on the mean user speed and the optimization requirements (Fig. 16). The $HHM_{c,(dB)}^{MM}$ parameter also affects the remainder performance measures, where the impact of varying $HHM_{c,(dB)}^{MM}$ on the mean UE transmit power is indicatively depicted in Fig. 17. Interestingly, as the $HHM_{c,(dB)}$ increases, the mean UE transmit power lowers for

both versions of the proposed algorithm (Fig. 17). Depending on the mean user speed and the HO context acquisition approach, however, there exists a $HHM_{c,(dB)}^{MM}$ value above which a degraded performance is observed. Similar results were derived for the remainder performance measures as well, indicating that the $HHM_{c,(dB)}^{MM}$ can be used to optimize the proposed algorithm with respect to a particular performance measure/target.

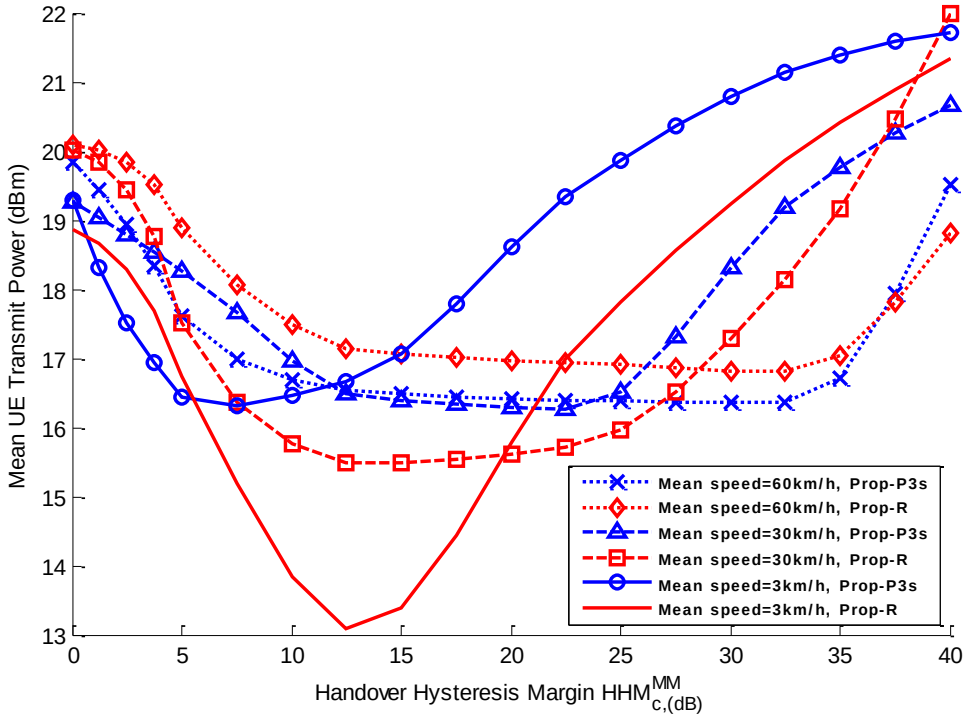

Figure 17: Mean UE transmit power vs. the Handover Hysteresis Margin $HHM_{c,(dB)}^{MM}$

7. CONCLUSION

An advanced mobility management approach for the two-tier LTE-Advanced network has been introduced in this paper, which jointly considers the impact of user mobility, interference, and power consumption. The proposed approach is based on the exchange and utilization of standard signaling quality measurements and the employment of energy-efficient interference-aware HO decision making. A novel HO decision algorithm has been proposed, and a detailed analysis has been provided with regards to the network signaling procedure for employing it. Two different signaling approaches have been identified, depending on whether a network entity maintains and disseminates the required HO decision context, or not. Extensive system-level simulation results have shown that compared to existing approaches, the proposed approach greatly reduces the mean UE and cell transmit power, lowers the mean UE energy expenditure per bit and UE interference, and enhances the system capacity, at the cost of moderate increase of network signaling. Although the reactive version of the proposed algorithm has shown to increase the X2 signaling and the mean cell interference, owing to the substantially increased femtocell utilization, the proactive version of the proposed algorithm is shown to attain similar X2 signaling and mean cell interference performance to that of the competing algorithms. The impact of the HHM parameter has also been investigated and it has been shown that depending on the mean user speed and the optimization requirements, a higher HHM value can be used to optimize the proposed algorithm's performance with respect to a particular performance measure/target.

LIST OF ACRONYMS

3rd Generation Partnership Project	3GPP
Access Network Discovery and Selection Function	ANDSF
Carrier Aggregation	CA
Closed Subscriber Group	CSG
Coordinated Multipoint	CoMP
Core Network	CN
Decibels	dB
Downlink	DL
Effective SINR mapping	ESM
Evolved Node B	eNB
Handover	HO
Handover Hysteresis Margin	HHM
Home eNB	HeNB
Information Element	IE
International Mobile Telecommunications	IMT
International Telecommunication Union	ITU
Long Term Evolution – Advanced	LTE-A
Mobility Management Entity	MME
Multiple-input multiple-output	MIMO
Quality of Service	QoS
Radio-Frequency	RF
Received Interference Power	RIP
Received Signal Strength	RSS
Received Signal Strength Indicator	RSSI
Reference Signal Received Power	RSRP
Reference Signal Received Quality	RSRQ
Reference Signals	RS
Resource Block	RB
Signal to Interference plus Noise Ratio	SINR
Strongest Cell	SC
Time To Trigger	TTT
Uplink	UL
User Equipment	UE

ACKNOWLEDGMENT

This paper has been partially funded by the CROSSFIRE (MITN 317126), CO2GREEN (TEC2010-20823), GREENET (PEOPLE 264759) projects, and Greek national funds through the Operational Program "Education and Lifelong Learning" of the National Strategic Reference Framework (NSRF) - Research Funding Program: Heracleitus II.

REFERENCES

[1] 3GPP, "Evolved Universal Terrestrial Radio Access (E-UTRA) and Evolved Universal Terrestrial Radio Access Network (E-UTRAN); Overall description", TS 36.300 V12.0.0, Jan. 2014.

[2] S. Parkvall, A. Furuskaär, E. Dahlman, "Evolution of LTE toward IMT-advanced", IEEE Communications Magazine, vol.49, no.2, pp.84-91, Feb. 2011.
[3] A.Ghosh, R. Ratasuk, B. Mondal, N. Mangalvedhe, T. Thomas, "LTE-advanced: next-generation wireless broadband technology", IEEE Wireless Communications, vol.17, no.3, pp.10-22, June 2010.
[4] J. G. Andrews, H. Claussen, M. Dohler, S. Rangan, M. C. Reed, "Femtocells: Past, Present, and Future", IEEE J. on Sel. Areas in Comm., vol.30, no.3, pp.497-508, Apr. 2012
[5] D. Xenakis, N. Passas, L. Merakos, C. Verikoukis, "Mobility Management for Femtocells in LTE-Advanced: Key Aspects and Survey of Handover Decision Algorithms," IEEE Comm. Surveys & Tut., vol.16, no.1, pp.64-91, First Quarter 2014.
[6] H. Leem, S. Y. Baek, D. K. Sung, "The Effects of Cell Size on Energy Saving, System Capacity, and Per-Energy Capacity", IEEE Wireless Communications and Networking Conf., pp.1-6, Apr. 2010.
[7] F. Cao, Z. Fan, "The tradeoff between energy efficiency and system performance of femtocell deployment", The 7th Internat. Symposium on Wirel. Commun. Syst. (ISWCS), pp.315-319, Sept. 2010.
[8] I. Ashraf, L.T.W. Ho, H. Claussen, "Improving Energy Efficiency of Femtocell Base Stations Via User Activity Detection", IEEE Wireless Commun. and Networking Conf. 2010, pp.1-5, Apr. 2010.
[9] Small Cell Forum, "Interference Management in OFDMA Femtocells", Small Cell Forum, Mar. 2010.
[10] M. Iwamura, K. Etemad, Mo-Han Fong, R. Nory, R. Love, "Carrier aggregation framework in 3GPP LTE-advanced", IEEE Communications Magazine, vol.48, no.8, pp.60-67, Aug. 2010.
[11] Q. Li, G. Li, W. Lee, M. Lee, D. Mazzarese, B. Clerckx, Z. Li, "MIMO techniques in WiMAX and LTE: a feature overview", IEEE Communications Magazine, vol.48, no.5, pp.86-92, May 2010.
[12] K. Loa, C. Wu, S. Sheu, Y. Yuan, M. Chion, D. Huo, L. Xu, "IMT-advanced relay standards", IEEE Communications Magazine, vol.48, no.8, pp.40-48, Aug. 2010.
[13] J. Zhang, G. de la Roche, "Femtocells: technologies and deployment", John Wiley & Sons Ltd, ISBN 978-0-470-74298-3, 2010.
[14] Y. Kim, S. Lee, D. Hong, "Performance Analysis of Two-Tier Femtocell Networks with Outage Constraints", IEEE Trans. on Wireless Commun., vol.9, no.9, pp.2695-2700, Sept. 2010.
[15] G. Boudreau, J. Panicker, N. Guo, R. Chang, N. Wang, S. Vrzic, "Interference coordination and cancellation for 4G networks", IEEE Communications Magazine, vol.47, no.4, pp.74-81, Apr. 2009.
[16] M. Kim, H.W. Je, F.A. Tobagi, "Cross-Tier Interference Mitigation for Two-Tier OFDMA Femtocell Networks with Limited Macrocell Information", 2010 IEEE Global Telecommunications Conf. (GLOBECOM 2010), pp.1-5, Dec. 2010.
[17] D. Lopez-Perez, A. Valcarce, G. de la Roche, Jie Zhang, "OFDMA femtocells: A roadmap on interference avoidance", IEEE Communications Magazine, vol.47, no.9, pp.41-48, Sept. 2009.
[18] D. Lopez-Péréz, A. Ladányi, A. Juttner, Jie Zhang, "OFDMA Femtocells: Intracell Handover for Interference and Handover Mitigation in Two-Tier Networks", 2010 IEEE Wireless Communications and Networking Conf. (WCNC 2010), pp.1-6, Apr. 2010.
[19] M. Yavuz, F. Meshkati, S. Nanda, A. Pokhariyal, N. Johnson, B. Raghothaman, A. Richardson, "Interference management and performance analysis of UMTS/HSPA+ femtocells", IEEE Communications Magazine, vol.47, no.9, pp.102-109, Sept. 2009.
[20] K. Zheng, B. Fan, J. Liu, Y. Lin, W. Wang, "Interference coordination for OFDM-based multihop LTE-advanced networks", IEEE Wireless Communications, vol.18, no.1, pp.54-63, Feb. 2011.
[21] V. Chandrasekhar, J.G. Andrews, T. Muharemovic, Z. Shen, A. Gatherer, "Power control in two-tier femtocell networks", IEEE Trans. on Wireless Commun., vol.8, no.8, pp.4316-4328, Aug. 2009.
[22] H. Jo, C. Mun, J. Moon, J. Yook, "Interference mitigation using uplink power control for two-tier femtocell networks", IEEE Trans. on Wireless Commun., vol.8, no.10, pp.4906-4910, Oct. 2009.
[23] A. Galindo-Serrano, L. Giupponi, M. Dohler, "Cognition and Docition in OFDMA-Based Femtocell Networks", 2010 IEEE Global Telecommunications Conf. (GLOBECOM 2010), pp.1-6, Dec. 2010.
[24] S. Park, W. Seo, Y. Kim, S. Lim, D. Hong, "Beam Subset Selection Strategy for Interference Reduction in Two-Tier Femtocell Networks", IEEE Trans. on Wirel. Commun. vol.9, no.11, pp.3440-3449, Nov. 2010.

[25] W. Shaohong, Z. Xin, Z. Ruiming, Y. Zhiwei, F. Yinglong, Y. Dacheng, "Handover Study Concerning Mobility in the Two-Hierarchy Network", IEEE 69th Vehic. Technology Conf. (VTC), pp.1-5, Apr. 2009.
[26] A. Ulvan, R. Bestak, M. Ulvan, "Handover Scenario and Procedure in LTE-based Femtocell Networks", The 4th International Conf. on Mobile Ubiquitous Comput., Syst., Serv. and Technolog., Oct. 2010.
[27] Z. Becvar, P.Mach, "Adaptive Hysteresis Margin for Handover in Femtocell Networks", 6th International Conf. on Wireless and Mobile Communications, pp.256-261, Sept. 2010.
[28] J. Chang, Y. Li, S. Feng, H. Wang, C. Sun, P. Zhang, "A Fractional Soft Handover Scheme for 3GPP LTE-Advanced System", 2009 IEEE International Conf. on Comm. (ICC 2009), pp.1-5, June 2009.
[29] D. Lopez-Péréz, A. Ladányi, A. Ju□ttner, J. Zhang, "OFDMA Femtocells: Intracell Handover for Interference and Handover Mitigation in Two-Tier Networks", 2010 IEEE Wireless Communications and Networking Conf. (WCNC 2010), pp.1-6, Apr. 2010.
[30] H. Zhang, X. Wen, B. Wang, W. Zheng, Yong Sun, "A Novel Handover Mechanism Between Femtocell and Macrocell for LTE Based Networks", Second International Conf. on Communication Software and Networks 2010 (ICCSN 2010), pp.228-231, Feb. 2010.
[31] H. Zhang, W. Ma, W. Li, W. Zheng, X. Wen, C. Jiang, "Signalling Cost Evaluation of Handover Management Schemes in LTE-Advanced Femtocell", IEEE 73rd Vehic. Techn. Conf., pp.1-5, May 2011.
[32] U. Narayanan, J. Xie, "Signaling Cost Analysis of Handoffs in a Mixed IPv4/IPv6 Mobile Environment", IEEE Global Telecommunications Conf. 2007 (GLOBECOM 2007), pp.1792-1796, Nov. 2007.
[33] S. Oh, H. Kim, B. Ryu, N. Park, "Inbound Mobility Management on LTE-Advanced Femtocell Topology Using X2 Interface", 2011 Proceed. of 20th Intern. Conf. on Comp. Comm. and Net., pp.1-5, Aug. 2011.
[34] D. Xenakis, N. Passas, and C. Verikoukis, "“An Energy-Centric Handover Decision Algorithm for the Integrated LTE Macrocell - Femtocell Network Computer Communications”, Comp.Comm., Elsevier, vol. 35, is. 14, pp. 1684-1694, Aug. 2012.
[35] D. Xenakis, N. Passas, and C. Verikoukis, "A Novel Handover Decision Policy for Reducing Power Transmissions in the two-tier LTE network", IEEE International Communications Conference (IEEE ICC) 2012, vol., no., pp., June 2012.
[36] 3GPP, "Physical layer - Measurements", TS 36.214 V11.1.0, Dec. 2012.
[37] S. Sesia, I. Toufik, M. Baker, “LTE – The UMTS Long Term Evolution: From Theory to Practice”, John Wiley & Sons, ISBN: 978-0-470-69716-0, 2009.
[38] 3GPP, “X2 application protocol (X2AP)”, TS 36.423 V12.1.0,Mar. 2014.
[39] 3GPP, “Radio Resource Control (RRC); Protocol specification”, TS 36.331 V12.1.0, Mar. 2014.
[40] 3GPP, “Access to the 3GPP Evolved Packet Core (EPC) via non-3GPP access networks; Stage 3”, TS 24.302 V10.6.0, Dec. 2011.
[41] 3GPP, “S1 Application Protocol (S1AP)”, TS 36.413 V12.1.0,Mar. 2014.

*Author Biography

CURRICULA VITAE OF THE AUTHORS

Dionysis Xenakis received his B.Sc. degree in Computer Science in 2007, his M.Sc. degree in Communications Systems and Networks in 2009, while he is currently pursuing his Ph.D. degree at the Department of Informatics and Telecommunications - University of Athens, Greece. In 2008, he received the M.Sc. Excellence Award in the field of Networks and Communication Systems from the same department. Dionysis participated in various FP7 research projects, including PHYDYAS, C2POWER, CROSSFIRE and SMART-NRG. He is a co-author of 8 conference papers, 4 journals papers, and 3 book chapters, while he has also been a reviewer in numerous peer-reviewed conferences and journals. From 2012, he has served as a keynote speaker in various well-established training and publication activities, including the 1st Femto Winter School (2012), FP7 ICT-Acropolis (NoE) Winter School (2013), and the 1st FP7 MITN-CROSSFIRE Seminar (2014). Dionysis has served as TPC of various conferences flagged by IEEE, e.g., CAMAD and HealthCom, as well as the reviewer in several peer reviewed conferences, e.g., IEEE ICC, IEEE Globecom, and journals, e.g., IEEE Transactions on Communications, IEEE Transactions on Wireless Communications, IEEE Communications Surveys & Tutoriasl, and Elsevier ComNet, Elsevier ComCom/ His current research interests include HetNets, D2D communications and green mobility management. Dionysis is currently an IEEE student member, member of the Communication Network Laboratory / University of Athens - Greece, and member of the Green Adaptive and Intelligent Networking Group / University of Athens - Greece.

Dr. Passas received his Diploma (honors) from the Department of Computer Engineering, University of Patras, Greece, and his Ph.D. degree from the Department of Informatics and Telecommunications, University of Athens, Greece, in 1992 and 1997, respectively. From 1992 to 1995 he was a research engineer at the Greek National Research Center "Demokritos". Since 1995, he has been with the Communication Networks Laboratory of the University of Athens, working as a sessional lecturer and senior researcher in a number of national and European research projects. He has also served as a guest editor and technical program committee member in prestigious magazines and conferences, such as IEEE Wireless Communications Magazine, Wireless Communications and Mobile Computing Journal, IEEE Vehicular Technology Conference, IEEE PIMRC, IEEE Globecom, etc. Dr. Passas has published more than 150 papers in peer-reviewed journals and international conferences and has also published 1 book and 7 book chapters. His research interests are in the area of mobile network architectures and protocols. He is particularly interested in QoS for wireless networks, medium access control, and mobility management. Dr. Passas is a member of the IEEE and a member of the Technical Chamber of Greece.

Prof. Lazaros Merakos received the Diploma in Electrical and Mechanical Engineering from the National Technical University of Athens, Athens, Greece, in 1978, and the M.S. and Ph.D. degrees in Electrical Engineering from the State University of New York, Buffalo, in 1981 and 1984, respectively. From 1983 to 1986, he was on the faculty of the Electrical Engineering and Computer Science Department, University of Connecticut, Storrs. From 1986 to 1994, he was on the faculty of the Electrical and Computer Engineering Department, Northeastern University, Boston, MA. During the period 1993–1994, he served as Director of the Communications and Digital Processing Research Center, Northeastern University. During the summers of 1990 and 1991, he was a Visiting Scientist at the IBM T. J. Watson Research Center, Yorktown Heights, NY. In 1994, he joined the faculty of the University of Athens, Athens, Greece, where he is presently a Professor in the Department of Informatics and Telecommunications, and Scientific Director of the Networks Operations and Management Center. His research interests are in the design and performance analysis of communication networks, and wireless/mobile communication systems and services. He has authored more than 200 papers in the above areas. He has served as the scientific director of the Communication Networks Laboratory of the University of Athens in numerous research projects, including the projects RAINBOW, WAND, MOBIVAS, WINE, EURO-CITI, POLOS, ANWIRE, E2R, E2RII, E3, Self-NET funded by the European Union. Dr. Merakos is chairman of the board of the Greek Schools Network, and member of the board of the National Research Network of Greece. In

1994, he received the Guanella Award for the Best Paper presented at the International Zurich Seminar on Mobile Communications.

Christos Verikoukis received degree in Physics and M.Sc. in Telecommunications Engineering from the Aristotle University of Thessaloniki in 1994 and 1997, respectively. He got his Ph.D. from the Technical University of Catalonia in 2000. Since February 2004, he is a senior research associate in Telecommunications Technological Centre of Catalonia (CTTC). Before joining CTTC, he was research associate and projects coordinator in the Southeastern Europe Telecommunications & Informatics Research Institute in Greece. He has been involved in several European (FP5 IST, FP6 IST & Marie-Curie, FP7 ICT & People, EUREKA) and national (in Spain and in Greece) research funded projects, while in some of them he has served at the Project or the Technical Manager. He has published over 100 journal and conference A. Antonopoulos et al. / Ad Hoc Networks 11 (2013) 190–200 199 papers, 10 chapters in different books and 2 books. His research interests include MAC protocols, RRM algorithms, cross-layer techniques, cooperative and cognitive communications for wireless systems.

PHOTOS OF THE AUTHORS